HHS Public Access

Author manuscript

Brain Stimul. Author manuscript; available in PMC 2021 June 20.

Published in final edited form as:

Brain Stimul. 2020 ; 13(5): 1333–1348. doi:10.1016/j.brs.2020.07.002.

Non-invasive vagal nerve stimulation decreases brain activity during trauma scripts

Matthew T. Wittbrodt[a,*], **Nil Z. Gurel**[b], **Jonathon A. Nye**[c], **Stacy Ladd**[a], **Md Mobashir H. Shandhi**[b], **Minxuan Huang**[d], **Amit J. Shah**[e,f], **Bradley D. Pearce**[c], **Zuhayr S. Alam**[a], **Mark H. Rapaport**[a], **Nancy Murrah**[c], **Yi-An Ko**[g], **Ammer A. Haffer**[d], **Lucy H. Shallenberger**[c], **Viola Vaccarino**[c,e], **Omer T. Inan**[b,h], **J. Douglas Bremner**[a,c,f]

[a]Department of Psychiatry and Behavioral Sciences, Emory University School of Medicine, Atlanta, GA, USA

[b]Department of Electrical and Computer Engineering, Georgia Institute of Technology, Atlanta, GA, USA

[c]Department of Radiology, Emory University School of Medicine, Atlanta, GA, USA

[d]Department of Epidemiology, Rollins School of Public Health, Emory University, Atlanta, GA, USA

[e]Department of Medicine (Cardiology), Emory University School of Medicine, Atlanta, GA, USA

[f]Atlanta VA Medical Center, Decatur, GA, USA

[g]Department of Biostatistics and Bioinformatics, Rollins School of Public Health, Emory University, Atlanta, GA, USA

[h]Wallace H. Coulter Department of Biomedical Engineering, Georgia Institute of Technology, Atlanta, GA, USA

Abstract

Background: Traumatic stress can have lasting effects on neurobiology and result in psychiatric conditions such as posttraumatic stress disorder (PTSD). We hypothesize that non-invasive cervical vagal nerve stimulation (nVNS) may alleviate trauma symptoms by reducing stress

[*]Corresponding author. 1821 Clifton Rd, Room 214, Atlanta, GA, 30307, USA. mattwittbrodt@emory.edu (M.T. Wittbrodt).

CRediT authorship contribution statement

Matthew T. Wittbrodt: Formal analysis, Writing - original draft, Writing - review & editing, Software, Visualization. **Nil Z. Gurel:** Writing - review & editing, Investigation, Data curation. **Jonathon A. Nye:** Formal analysis, Writing - review & editing, Supervision. **Stacy Ladd:** Investigation, Data curation. **Md Mobashir H. Shandhi:** Investigation, Data curation. **Minxuan Huang:** Investigation, Data curation. **Amit J. Shah:** Writing - review & editing, Supervision. **Bradley D. Pearce:** Writing - review & editing, Resources, Methodology. **Zuhayr S. Alam:** Formal analysis, Data curation. **Mark H. Rapaport:** Writing - review & editing, Supervision. **Nancy Murrah:** Investigation, Data curation, Project administration, Methodology. **Yi-An Ko:** Formal analysis, Data curation. **Ammer A. Haffer:** Investigation. **Lucy H. Shallenberger:** Project administration, Resources, Methodology. **Viola Vaccarino:** Writing - review & editing, Supervision, Funding acquisition, Methodology, Conceptualization. **Omer T. Inan:** Writing - review & editing, Supervision, Funding acquisition, Methodology, Conceptualization, Project administration. **J. Douglas Bremner:** Formal analysis, Writing - original draft, Writing - review & editing, Project administration, Supervision, Resources, Funding acquisition, Methodology, Conceptualization.

Appendix A. Supplementary data

Supplementary data to this article can be found online at https://doi.org/10.1016/j.brs.2020.07.002.

sympathetic reactivity. This study examined how nVNS alters neural responses to personalized traumatic scripts.

Methods: Nineteen participants who had experienced trauma but did not have the diagnosis of PTSD completed this double-blind sham-controlled study. In three sequential time blocks, personalized traumatic scripts were presented to participants immediately followed by either sham stimulation (n = 8; 0–14 V, 0.2 Hz, pulse width = 5s) or active nVNS (n = 11; 0–30 V, 25 Hz, pulse width = 40 ms). Brain activity during traumatic scripts was assessed using High Resolution Positron Emission Tomography (HR-PET) with radiolabeled water to measure brain blood flow.

Results: Traumatic scripts resulted in significant activations within the bilateral medial and orbital prefrontal cortex, premotor cortex, anterior cingulate, thalamus, insula, hippocampus, right amygdala, and right putamen. Greater activation was observed during sham stimulation compared to nVNS within the bilateral prefrontal and orbitofrontal cortex, premotor cortex, temporal lobe, parahippocampal gyrus, insula, and left anterior cingulate. During the first exposure to the trauma scripts, greater activations were found in the motor cortices and ventral visual stream whereas prefrontal cortex and anterior cingulate activations were more predominant with later script presentations for those subjects receiving sham stimulation.

Conclusion: nVNS decreases neural reactivity to an emotional stressor in limbic and other brain areas involved in stress, with changes over repeated exposures suggesting a shift from scene appraisal to cognitively processing the emotional event.

Keywords

Vagal nerve stimulation; PTSD; Trauma scripts; Stress; Prefrontal cortex; Insula

Introduction

Traumatic stress is known to have lasting effects on neurobiology [1,2] and, in at risk individuals, can result in psychiatric conditions such as posttraumatic stress disorder (PTSD) [3]. During acute traumatic stress exposure, sympathetic nervous system (SNS) activity increases [1,4,5], resulting in a neuroendocrinological cascade with potentially deleterious neural consequences [6–8]. Heightened sympathetic response either during an acute traumatic event as well as chronic hyperarousal is a hallmark of PTSD [6], and therefore minimizing SNS reactivity to stress may be an effective avenue for treatment. One such approach, neuromodulation, has been previously effective in mitigating the acute stress response [5,9], enhancing the anti-inflammatory response [10], providing neuroprotection [11], improving depression symptoms [12–15], aiding recovery following traumatic injury [16,17], and enhancing cognitive recovery or fear extinction [18–20].

One neuromodulation technique with great promise to mitigate exacerbated SNS reactivity is the electrical stimulation of the vagus nerve (i.e., vagal nerve stimulation or VNS). VNS, administered using an implantable device delivering current to the vagus through a cuff electrode, has previously been observed to mitigate the stress response through lessened peripheral inflammatory and cardiovascular responses in addition to increasing activity in brain areas with functional connections to the vagus nerve [5,21–26]. Lessened sympathetic response appears to results from stimulating the afferent fibers of the vagus nerve which

activates the nucleus tractus solitarius (NTS) in the medulla oblongata, activating and the locus coeruleus in the pons [27], and eventually relays to emotional and stress-responsive areas in the brain such as the insula [28]. Activation of the locus coeruleus stimulates the brain noradrenergic system [29], which appears necessary for the therapeutic benefits of VNS [30]. Secondly, the decreased inflammatory response with VNS appears to result from NTS mediated activation of the dorsal motor nucleus and subsequent efferent pathway activation to the celiac ganglion, inhibiting cytokine production from the spleen [31]. In addition, VNS appears to improve memory when applied during learning [32–34], potentially through increased sensory gating or effects on neuroplasticity [35].

New non-invasive transcutaneous VNS (nVNS) devices have been developed that are safe, cost-effective, and portable, potentially facilitating broader adoption (e.g., at-home) and thus eliminates some of the previous limitations of implantable VNS such as high cost, surgery, and introduction of a foreign object into the patient [36,37]. Recent modeling [38] and electrophysiological [39] studies have observed that cervical (neck) and auricular nVNS stimulates afferent fibers of the vagus nerve similar to implantable VNS [40] along with the NTS [41–44]. Despite these theoretical benefits and proof-of-concept studies, little evidence exists regarding the mechanism of action [24,37] of nVNS. Resting neuroimaging studies in healthy adults receiving cymba conchae stimulation in the ear (auricular vagal branch) found increased activations within the insula, paracentral lobule, somatosensory cortex, thalamus, contralateral amygdala, and medulla with deactivations observed in the hippocampus and hypothalamus [42,44]. A subsequent resting auricular nVNS study [43] observed similar findings, although nVNS activated rather than deactivated the hypothalamus. Studies employing cervical nVNS have observed activation within a cortical network of the insula, caudate, postcentral gyrus, anterior cingulate, prefrontal cortex, cerebellum, basal ganglia, thalamus, and the primary sensory cortex [41], while deactivating visual areas and the hippocampus.

However, little is known about how cervical nVNS alters neural activation patterns in response to an emotional stressor such as listening to scripts of previous traumatic events. Traumatic scripts are known to produce an acute stress response and increase SNS activity in previously traumatized individuals with [6,45,46] and without [47,48] PTSD. Exposure to traumatic scripts activates neural areas repeatedly found to be altered with PTSD and related psychiatric disorders [6,45,49]: the amygdala, prefrontal cortex, anterior cingulate, hippocampus, and insula. Since, as described above, cervical nVNS is thought to decrease activity of SNS neural circuits [41–43], this study was designed to examine how cervical nVNS alters neural responses to traumatic scripts in trauma-exposed individuals without PTSD. We hypothesized that nVNS will decrease neural activity compared to a sham device in brain areas involved in the stress response, specifically within the amygdala, prefrontal cortex, anterior cingulate, hippocampus, and insula during exposure to personalized traumatic scripts.

Materials and methods

Participants

This study was approved by the institutional review boards of Emory University (#IRB00091171), Georgia Institute of Technology (#H17126), SPAWAR Systems Center Pacific, and the Department of Navy Human Research Protection Program (ClinicalTrials.gov # NCT02992899). It should be noted that, although the ClinicalTrials.gov study description included the neuroimaging methods presented in this study, brain activity findings were not listed as primary or secondary outcomes. All participants provided written and verbal informed consent before enrolling in the study. Fig. 1A presents the Consolidated Standards of Reporting Trials (CONSORT) for this study. For the 46 individuals screened for eligibility, six declined to participate and 13 did not meet the inclusion criteria. The 27 remaining participants were randomized using an online tool into either sham stimulation or nVNS groups. Eight participants were excluded from analysis due to equipment malfunction or withdrawals. The remaining 19 participants were included in the analysis with n = 11 receiving nVNS and n = 8 receiving sham stimulation (Table 1).

Participants were healthy adults between 18 and 65 y with a history of psychological trauma (as defined by the Diagnostic and Statistical Manual (DSM-5) [50]; details of trauma presented in Supplementary Table 1) but no current diagnosis of PTSD or major psychiatric disorder (e.g., schizophrenia, schizoaffective disorder, bipolar disorder, severe major depression, bulimia or anorexia). The traumatic memory details of one participant was lost due to technical error. Among the remaining eighteen traumatic memories, the most common traumas were related to molestation or sexual abuse (28%), illness, injury, or death of a family member (22%), personal injury including victim of assault and/or robbery (22%), car accidents or house fire (22%), illness, injury, or death of nonfamily individuals (17%), and emotional abuse from family or peers (17%). The Clinician Administered PTSD Scale (CAPS-5) was administered by a trained member of the research staff to confirm absence of current PTSD using previously validated scoring [51]. The Early Childhood Trauma Inventory Self-Report [52,53] (64 total items) and a preliminary shortened version of the Adulthood Trauma Inventory [54] (16 total items) were administered to examine trauma load throughout the lifespan. The Structured Clinical Interview for DSM-IV (SCID) was also used to determine the presence of psychiatric disorders [55]. Three participants (17%) met criteria for a past history of major depression, one participant (6%) reported past PTSD, and one (6%) experienced past panic disorder. No subjects met criteria for current or past alcohol or substance use disorder. Exclusion criteria included: pregnancy, traumatic brain injury, meningitis, active implanted devices, evidence or history of serious medical or neurological illness, post-menopausal status, positive toxicology screen, and carotid atherosclerosis.

Study design

Data collection occurred between May 2017 and October 2018 at Emory University School of Medicine. nVNS and Sham devices were delivered to the research staff pre-numbered by the manufacturer (*ElectroCore, Basking Ridge, NJ*) and they were distributed by an individual not involved in any other aspect of the protocol. Research staff conducting

enrollment and data collection were masked to stimulus condition. Only the research staff conducting data analysis, but not involved in data collection, knew the stimulus assignment.

During an initial screening, participants completed the psychiatric interview and gave a written history of traumatic experiences. A 60-s personalized traumatic script was developed and recorded by a member of the research team for each subject similar to previous methods [45]. On the second visit, subjects participated in a high-resolution positron emission tomography (HR-PET) scan session during which they listened to traumatic and neutral scripts (Fig. 1B). Neutral scripts were employed to induce neutral-to-positive affective responses in participants. Scripts were delivered using headphones to participants who were supine in HR-PET scanner. nVNS or sham was applied immediately following the personalized script to the left side of the neck for 2 min by research personal. The length of stimulation was automatically controlled by the device. Two HR-PET scans were also completed using nVNS/sham stimulation with the subject at rest with eyes open, and not performing a task or listening to a script.

Non-invasive vagus nerve stimulation

All stimulation (nVNS or sham) was administered with handheld devices (*GammaCore, ElectroCore, Basking Ridge, NJ*) using collar electrodes applied to the left side of the neck for 120 s. The appearance and operation of the nVNS and sham devices were identical. The location for placement of collar electrodes on the carotid and application of conductive gel to maintain adequate skin-electrode contact has been previously described in detail [39]. nVNS devices produced an AC voltage signal consisting of five 5 kHz sine bursts (1 ms of five sine waves; pulse width = 40 ms) repeating at a rate of 25 Hz. The sham devices produce an AC biphasic voltage signal consisting of 0.2 Hz square pulses (pulse width = 5 s) eliciting a mild sensation similar to nVNS but without stimulating the vagus nerve. nVNS stimulation intensity was adjustable and ranged from 0 to 5 au (arbitrary units) with a corresponding peak output ranging from 0 to 30 V (~0–60 mA) for active nVNS and 0–14 V (~0–60 mA) for sham. Stimulation periods started with gradually increasing intensity until participants instructed to stop; stimulation intensity was therefore the maximum tolerable without pain. The maximum tolerable amplitude level was 3 ± 0.9 au for nVNS and all participants with sham used an intensity of 5. In our larger sample not restricted by HR-PET availability [5], the mean sham stimulation (12.8 V) was below the 14 V maximum for the sham device, indicating the unanimous selection of 5 au in this cohort was a sampling artifact. The research staff, who were blinded to stimulation type, confirmed all participants perceived the stimulation.

Neuroimaging and analysis

HR-PET imaging was completed using a High Resolution Research Tomograph (HR-PET) (*CTI, Knoxville, TN*) [56]. During each scan, participants lay supine in the scanner and were instructed to be as still as possible. Brain perfusion was assessed to quantify regional voxel-wise activity responses (2 mm spatial resolution) to the traumatic and neutral scripts. Five seconds before each script presentation, 20 mCi of radio-labeled water (H_2O^{15}), produced in an on-site cyclotron, was intravenously administrated before a 2-min HR-PET scan was collected following to measure brain blood perfusion. Script presentation began concurrently

with HR-PET scan initiation. Radio-labeled water was injected 5 s before the stimulation period for the nVNS-only scans (scan numbers five and six, Fig. 1B).

HR-PET images were analyzed similarly to previous research [57] using statistical parametrical mapping (SPM12; www.fil.ion.ucl.ac.uk/spm). First, using the fourteen individual scans, a mean intensity image was generated. The individual scans were spatially normalized to the mean intensity image, transformed into a common anatomical space (SPM PET Template), smoothed using a three-dimensional Gaussian filter at 5-mm full width half maximum, and lastly normalized to whole brain activity. First level models were computed using the neutral script scan and traumatic script conditions. This model was grand mean scaled, estimated, and contrasts computed for activation (traumatic – neutral scripts) and deactivation (neutral – traumatic scripts). For stimulation only scans (scan numbers five and six, Fig. 1), a one sample *t*-test was completed to examine areas of elevated brain activity during the scan. Second level (between-participant) analyses were completed using contrast images from the first level analysis and grouped by stimulation type. In addition, an analysis was completed across three trauma script blocks (TSB1–3; Fig. 1). Each TSB consisted of two trauma and neutral scripts except for TSB1 where the first trauma script was omitted because it preceded any stimulation.

Statistical analysis

Normality of data was assessed using the Shapiro-Wilk test within R (*v3.4.0;* www.r-project.org). Comparisons between nVNS and sham groups were completed using a two-sample *t*-test or Mann-Whitney-Wilcoxon test for continuous and Fisher's exact test for discrete variables, respectively. For regional brain blood flow analyses (HR-PET), comparison contrasts examining areas of greater activation and deactivation between nVNS and sham were encoded according to previous guidelines [58] resulting in between-group t-statistic brain maps. Significant voxel clusters for main brain analyses were identified using a threshold of $p < 0.005$ (uncorrected) and minimum voxel cluster size of eleven to minimize Type I and Type II errors in neuroimaging research [59,60]. For trauma script block analysis, p values were Bonferroni corrected for multiple comparisons, yielding an alpha of 0.0025 ($n = 2$) across time points and 0.0017 ($n = 3$) between stimulation types at each trauma script block. In addition, the trauma script block analyses were masked with the overall activity maps. Significant cluster peaks were identified using the distance from the anterior commissure with x, y, and z coordinates transformed from Montreal Neurological Institute (MNI) space to those of the Talairach stereotaxic atlas [61]. Cluster peaks were also identified using Brodmann Areas (BA) sourced from the Talairach daemon (www.talairach.org). The *a priori* α level for non-brain imaging data was chosen at 0.05. All data are presented as mean ± SD.

Results

Demographics

There were no significant differences between participants receiving nVNS or sham on any demographic, descriptive, or clinical variable (Table 1). nVNS and sham also demonstrated similar PTSD checklist scores which were below the threshold for current PTSD (Table 1).

Brain activity during the trauma script periods

Fig. 2 presents the overall patterns of activation and deactivation, collapsed across stimulation type, during exposure to the traumatic scripts. In general, trauma scripts elevated brain activity within the medial and orbital frontal lobe and limbic areas and decreased activity within the occipital lobe and cerebellum. Specifically, across the entire sample, trauma scripts resulted in significant ($p < 0.005$) activations within the bilateral medial and orbital prefrontal cortex, premotor cortex, anterior cingulate, thalamus, insula, hippocampus, pallidum, temporal lobe, parietal lobe, cerebellum, right amygdala, and right putamen. In addition, across the whole sample trauma scripts elicited significant deactivations ($p < 0.005$) within the bilateral cerebellum, parietal precuneus, occipital lobe, subgenual anterior cingulate, temporal lobe, superior and middle frontal gyrus, and left caudate.

The application of nVNS throughout the traumatic script presentation mitigated brain activity compared to sham (Fig. 3 and Tables 2–3), specifically within the medial and orbital frontal lobe. Compared to nVNS, sham elicited significantly ($p < 0.005$) greater brain activations during trauma scripts within the bilateral frontal lobe (BA 10, 11, 45, 47; prefrontal and orbitofrontal cortices, Broca's area), premotor cortex (BA 6), temporal lobe (BA 20–22, 42; fusiform, inferior, middle, superior gyrus), parietal precuneus and angular gyrus (BA 7, 19, 39), parahippocampal gyrus, thalamus, insula, cerebellum, right occipital lobe (BA 18), and left anterior cingulate (BA 32). Listening to the trauma scripts elicited one cluster (voxel size = 20, peak Z = 3.38, Talairach Coordinates = −24, −38, −18) of significant deactivation during nVNS compared to sham stimulation within the left cerebellum. Compared to nVNS, sham elicited greater deactivations during the trauma scripts within the bilateral posterior cingulate (BA 29–31), bilateral occipital lobe (BA 17–19, 31; cuneus and lingual, inferior, middle gyri), bilateral prefrontal cortex (BA 5, 6, 9, 10, 46), bilateral temporal lobe (BA 21, 22, 39; middle, transverse, superior gyri), bilateral parietal lobe (BA 7, 40, 43; postcentral gyrus, precuneus, inferior lobule), right anterior cingulate (BA 10), and right cerebellum.

Trauma script block analysis

The overall timeseries analysis found greater activations only during TSB3 compared to TSB2 within the frontoparietal areas and the putamen while greater deactivations successively appeared within occipital and temporal areas (Fig. 4, Table 4). Compared to TSB1, listening to the trauma scripts elicited greater ($p < 0.0025$) deactivation within the left inferior temporal gyrus (BA 20) and occipital cuneus (BA 18) during TSB2. Compared to TSB2, trauma scripts elicited greater ($p < 0.0025$) activations within the right postcentral parietal lobe (BA 1), right putamen, right superior temporal gyrus (BA 22), and left precentral gyrus (BA) and greater deactivations within the right superior temporal gyrus (BA 22), left middle temporal gyrus (BA 21), and left occipital cuneus (BA 31) during TSB3. Supplementary Table 2 and Supplementary Figure 1 describe the trauma script block changes with sham. No changes were observed from TSB1 to TSB2 ($p > 0.0025$). Compared to TSB2, hearing the trauma scripts elicited greater activations within right postcentral gyrus (BA 1), right caudate, bilateral claustrum, lateral prefrontal cortex (BA 40, 44, 46), and left posterior cingulate (BA 31) and deactivations within the right cerebellum and left occipital precuneus (BA 31) with sham stimulation. nVNS did not exhibit any changes in activation (p

> 0.0025) or deactivations between TSB1 and TSB2. Compared to TSB2, being exposed to the trauma scripts elicited significant ($p < 0.0025$) deactivation within the left parietal precuneus (BA 7), right posterior cingulate (BA 30), right hippocampus, and left middle temporal gyrus (BA 21) during TSB3.

During TSB1, sham elicited a general upregulation of stress-related brain areas compared to active nVNS (Figs. 5–6, Tables 5–6) while differences in TSB2 and TSB3 were more focal to the frontal and parietal lobes, respectively. Listening to trauma scripts caused greater activation for subjects undergoing sham stimulation compared to nVNS within the bilateral cerebellum, bilateral temporal lobe (inferior and fusiform gyrus; BA 20), bilateral prefrontal cortex (BA 10, 11, 46), right secondary motor cortex (BA 6), right parietal precuneus (BA 7), right insula, right anterior cingulate (BA 24), and bilateral parahippocampal gyrus during TSB1 (Fig. 5, Table 5). In addition, listening to the trauma scripts caused greater deactivation for subjects undergoing sham stimulation compared to nVNS within the right insula, left precentral gyrus (BA 9), bilateral inferior frontal gyrus (BA 45, 46), bilateral middle temporal lobe (BA 37), left anterior cingulate (BA 32), bilateral posterior cingulate (BA 30, 31), and right parahippocampal gyrus during TSB1. Listening to trauma scripts caused greater activation for subjects undergoing sham stimulation compared to nVNS within the right cerebellum, left inferior temporal cortex (BA 37), right medial temporal cortex (BA 21), Broca's area (BA 45), left visual eye field (BA 8), right dorsomedial perfrontal cortex (BA 9), right paracentral lobule (BA 5), and left dorsal anterior cingulate (BA 24) during TSB2. Additionally, listening to trauma scripts caused greater deactivation for subjects undergoing sham stimulation compared to nVNS in the bilateral insula, right parahippocampal gyrus, right thalamus, left cerebellum, left postcentral gyrus and precuneus (BA 7), bilateral premotor cortex (BA 6), right prefrontal cortex (BA 9,10, 44), and left superior temporal gyrus (BA 39) during TSB2. Listening to trauma scripts caused greater activation for subjects undergoing sham stimulation compared to nVNS within the left prefrontal cortex (BA 10, 46), right precentral gyus (BA 44), right inferior, superior, and postcentral parietal lobe (BA 7,19, 40), left somatosensory cortex (BA 5), right fusiform gyrus (BA 37), bilateral claustrum, and right caudate along with greater deactivations within the bilateral prefrontal cortex (BA 9, 10, 47), right anterior cingulate (BA 32), right superior temporal gyrus (BA 38), left occipital precuneus (BA 31), and right cerebellum during TSB3. Listening to trauma scripts caused greater activation for subjects undergoing nVNS compared to sham stimulation in the right precentral gyrus (16 voxels, BA 4) during TSB2; no differences ($p > 0.0017$) were observed during TSB1 and TSB2.

Sham stimulation vs. nVNS

Without trauma scripts, brain activity with sham remained elevated within the frontal lobe and limbic system (Fig. 7, Table 7) while nVNS resulted in greater activity within the occipital lobe and inferior frontal lobe. Participants receiving sham stimulation had significantly ($p < 0.005$) greater brain activity compared to nVNS within the bilateral anterior cingulate (BA 32), bilateral rostromedial and dorsomedial prefrontal cortex (BA 10; BA 8, 9), bilateral lateral oribitofrontal frontal cortex (BA 11, 47), bilateral parietal precuneus (BA 7), left paracentral lobule (BA 5), right somatosensory cortex (BA 2), left inferior parietal lobe (BA 40), bilateral middle temporal lobe (BA 20, 21), bilateral

cerebellum, left insula, and right occipital cuneus (BA 17). In contrast, participants receiving nVNS exhibited significantly ($p < 0.005$) greater brain activity compared to sham stimulation within the bilateral inferior frontal gyrus (BA 47), bilateral middle temporal gyrus (BA 21, 37), and left inferior occipital gyrus (BA 17; Fig. 7, Table 7).

Discussion

This study showed that nVNS compared to sham stimulation decreased activation in multiple limbic and stress-related brain areas associated with exposure to personalized traumatic scripts in traumatized individuals without current PTSD. Our trauma script block analysis suggests the blunted neural responses occur immediately upon traumatic script exposure and persist throughout the duration of emotional stress. During resting conditions (no traumatic script), nVNS also lowered brain activity within stress-response areas such as the anterior cingulate and frontal lobe. Taken together, the results of this study provide evidence that nVNS applied to the cervical branch of the vagus nerve is effective in lowering neural reactivity to personalized emotional stress and therefore may have utility as a treatment for many psychiatric disorders such as PTSD.

The primary finding of this study was that the application of nVNS following exposure to the personalize trauma scripts significantly reduced activity in select brain regions compared to a sham device. This is the first study to observe a dynamic change in neural responses during an emotional stressor. Listening to the personalized trauma scripts elicited similar brain activation patterns to what was previously reported in healthy traumatized individuals and patients with PTSD [46,62–68]: the bilateral prefrontal cortex, premotor cortex, anterior cingulate, insula, hippocampus, cerebellum, right amygdala, and right putamen. We believe these activations represent increased prefrontal lobe activity with additional upregulation of associated cortical networks [69]. In this study nVNS reduced brain activation in a multitude of brain areas that are similar to those reported in brain activity studies with auricular and cervical nVNS and seem to specifically activate parasympathetic networks leading to reduced reactivity with stress [41,43].

In addition to the large-scale effects, this study found evidence that emotion-specific neural networks were downregulated by nVNS. The largest area of lower activation while listening to the trauma scripts paired with nVNS compared to sham stimulation was located within the left rostromedial prefrontal cortex (BA 10) extending into the left dorsolateral prefrontal cortex (BA 46). Rostromedial prefrontal cortex activity increases when listening to trauma scripts and, in trauma-exposed individuals, appears to have functional connections to visual and autobiographical recall areas (hippocampus, temporal lobe, occipital lobe) [70]. The rostromedial prefrontal cortex also mediates changes in affect [71] and emotional appraisal (as opposed to cognitive appraisal) during autobiographical recall of personal traumatic events [72]. Dorsolateral prefrontal cortex (BA 46) is also active during traumatic autobiographical event recall [72] and is likely involved in appraisal of the emotional state [69], and is functionally connected to other areas (parietal cortex, middle temporal gyrus, motor areas, insula) with less activation when listening to trauma scripts paired with nVNS. Furthermore, the less rostromedial prefrontal cortex activity with concomitant pregenual anterior cingulate (BA 24) deactivation was found during autobiographical recall followed

by nVNS which suggests there is active inhibition of the emotional and cognitive centers of the anterior cingulate (BA 24) [70,73,74]. The left insula, which is associated with negative affect and is functionally connected to the prefrontal cortex was less active with nVNS compared to sham stimulation [69,71]. The insula and medial prefrontal cortex comprise are the areas of output to peripheral cardiovascular and autonomic responses and thus play an important role in regulation of the stress response [75]. Taken together, these results suggest personalized trauma scripts elicited the canonical pattern of emotionally responsive brain areas and the application of nVNS significantly diminished this response.

The second major finding of the present study was that nVNS suppresses emotionally responsive brain areas at different time points. This is important given the importance of understanding the temporal specificity of nVNS in the context of neuromodulation treatment for psychiatric disorders [76]. In animal models, invasive VNS produces a rapid excitation/inhibitory response within the forebrain [77] along with increased brain-derived neurotrophic factor in the hippocampus and norepinephrine concentration in prefrontal areas [78]. In humans, we have added to this literature by: (i) identifying sensitive physiological biomarkers indicating a lower stress response with nVNS [5] along with classifying sham/active stimulation [79] and (ii) observing evidence of stimulation in humans, as measured at the periphery, within 16 and 21 s with and without traumatic stress, respectively [80]. These combined efforts are supportive efforts to eventually allow for closed-loop stimulation via monitoring of peripheral signals.

The time-series data contained within this manuscript align with the sustained changes observed in with VNS such as neuroplasticity [81] and improved memory performance [32]. The first traumatic script exposure with nVNS resulted in decreased brain activation in a pattern appearing to indicate scene reconstruction as evidenced by upregulations of the ventral visual stream and motor areas compared to sham stimulation. While the trauma scripts did not include a visual stimulus, the left fusiform gyrus and parahippocampal gyrus were less activated with nVNS and thus may represent the reconstruction of subjects and environment during the traumatic event [82,83]. In addition, right posterior cingulate (BA 30) and other parietal areas were deactivated less with nVNS compared to sham stimulation which may indicate a decrease in the left-lateralized visual network which is related to visualizing autobiographical events [84,85]. Greater activation in motor areas has been found previously employing the trauma script paradigm in individuals with PTSD and may indicate poor fear response extinction [66].

During the second period of listening to the trauma script, the largest cluster of decreased activity with nVNS compared to sham stimulation occurred within the left pregenual anterior cingulate (BA 24) and in the left inferior temporal gyrus (BA 37). The pregenual anterior cingulate processes viscerosensory signals and activity is related to feelings of unpleasantness [69,86]. The pregenual anterior cingulate is also functionally connected to the rostromedial prefrontal cortex [69] which was also downregulated in the nVNS compared to sham stimulation group. We speculate that lower left inferior temporal gyrus activation following nVNS is independent from the rostromedial prefrontal cortex-pregenual anterior cingulate and, together with the third time point, indicate a prolonged period of lower emotional processing and feelings of unpleasantness compared to sham stimulation

[87]. This is further supported by lower brain activity with nVNS during the third trauma stimulation block occurring within the left lateral (BA 46) and rostromedial (BA 10) prefrontal cortex as well as functionally connected areas of the left inferior parietal lobe which process emotional regulation and autobiographical events [69]. In summary, the findings suggest that traumatic script exposure paired with nVNS initially was associated with a lower activation of brain areas that were likely involved in visualization of the stressful scene and mentally acting out motor responses to threat, with a later shift to less emotional processing of the event.

Taken together, the two major findings of this study indicate the potential for nVNS use a therapeutic tool. The current study showed that nVNS blocks the effects of reminders of traumatic stress on activation of the medial prefrontal cortex/anterior cingulate in traumatized individuals without PTSD. We have previously shown that traumatic reminders in non-PTSD trauma exposed individuals (e.g., combat veterans without PTSD) exposed to combat-related slides and sounds, results in an activation of medial prefrontal cortex/anterior cingulate [63], which we suggested was a normal brain response to emotionally arousing stimuli in which activation in this area led to suppression of amygdala function and hence excessive reactivity to stimuli that did not in fact represent a real threat, while PTSD patients in contrast failed to activate this area to the same degree and therefore had increased fear and physiological reactivity to what were in fact innocuous stimuli. The current findings suggest that nVNS blunts the responsivity of medial prefrontal cortex/anterior cingulate to traumatic reminders, suggesting that it modulates emotional responsivity of the brain, but how that translates to a treatment effect for PTSD, in which one in theory might hope for an enhancement of medial prefrontal cortex/anterior cingulate to promote inhibition of the amygdala [95–97], is not clear. While invasive VNS has repeatedly demonstrated the capacity to improve extinction in rodent models [18,88,89], the evidence supporting similar benefits with transcutaneous VNS in humans is less clear [90–93]. Understanding these discrepancies is an important tenant of future nVNS research, and therefore more studies are needed to understand the efficacy of nVNS in extinction paradigms including optimizing stimulation parameters. One reported limitation with transcutaneous VNS investigations has been the lack of a distinct physiological signal to demonstrate its efficacy [24]. Our recent work [5,79,80] has utilized novel cardiovascular biomarkers to identify candidate signals to demonstrate efficacy of nVNS. These findings, combined with the current results, could help provide stimulation feedback with prognostic value to improve efficacy of extinction therapy. nVNS has the potential to improve treatment strategies utilizing repeated exposure or other behaviors such as cognitive-behavioral therapy or mindfulness-based stress reduction which have shown to be effective in improving traumatic stress-related disorders such as PTSD [94]. Further work utilizing these sensitive novel physiological markers coupled with a therapeutic intervention are needed to better understand the potential clinical utility as nVNS.

Consistent with other studies, we found nVNS increased brain activity within the left occipital lobe [41] and bilateral inferior frontal gyrus [15,28,41–43] without the presence of personalized trauma scripts. We did not find increases in brain activity with nVNS in other areas previously reported under resting conditions [15,28,41–44,98] such as the insula and hippocampus, but the current study is not directly comparable given the previous exposure to

trauma scripts. The effects of trauma scripts can be persistent [68] and previous exposure likely precluded the measurement of a true resting state similar to the previous studies. Therefore, we believe our findings without trauma scripts are a function of the trauma script paradigm.

While this study presents novel findings regarding the influence of nVNS as a mechanism for reducing neural responses to emotional stress, we recognize there are some limitations to our work. First, we do not have a direct measurement of vagus nerve activity. A number of studies utilizing the same cervical nVNS device have found neural evidence supporting stimulation of the vagus with similar stimulation-specific sensory evoked potentials as implantable devices [39,99,100] and changes in power spectrum consistent with inhibitory electrical activity [35,101]. Regarding the sham device, participants were not asked what type of stimulation they received. These prompts should be asked in future investigations to understand potential biases in response patterns. Secondly, as alluded to above, the resting HR-PET scans without hearing neutral or personalized traumatic scripts were likely influenced by preceding trauma scripts and we cannot discern the isolate effects of nVNS alone similar to previous studies [41,42]. Third, the cross-sectional nature of this study precludes evidence of longer-term effects of transcutaneous cervical nVNS. We also acknowledge that this work needs to be replicated with a larger sample of subjects. Future studies should also assess the associations between neural responses during traumatic scripts, with and without nVNS, to changes in behavioral and physiological changes.

Conclusion

In conclusion, this study has provided novel findings about neural responses to nVNS while listening to personalized, emotionally stressful trauma scripts. We have demonstrated profound effects of nVNS in blunting the upregulation of neural responses elicited by trauma scripts. These effects were observed during all three exposures to trauma scripts in a pattern which may suggest that cervical nVNS decreases activity during both scene reconstruction and subsequent adverse emotional responses. We believe that future studies employing nVNS to enhance fear extinction as a treatment for PTSD or other emotional affective disorders might be fruitful.

Supplementary Material

Refer to Web version on PubMed Central for supplementary material.

Acknowledgments

This work was sponsored by the Defense Advanced Research Projects Agency (DARPA) Biological Technologies Office (BTO) Targeted Neuroplasticity Training (TNT) program through the Naval Information Warfare Center (NIWC) Cooperative Agreement No. N66001-16-4054. We acknowledge and thank Margie Jones, C.N.M.T. and Steve Rhodes, R.N., for their assistance with imaging analysis, patient assessments, and clinical research.

Declaration of competing interest

Dr. Bremner reported having funding support from ElectroCore LLC. No other authors report potential conflicts of interests.

Author declaration

We wish to draw the attention of the Editor to the following fact which may be considered as potential conflict of interest to this work: Author J. Douglas Bremner reported having funding support from ElectroCore LLC. For other authors, there are no known conflicts of interest associated with this publication and there has been no significant financial support for this work that could have influenced its outcome.

We confirm that the manuscript has been read and approved by all named authors and that there are no other persons who satisfied the criteria for authorship but are not listed. We further confirm that the order of authors listed in the manuscript has been approved by all of us.

We confirm that we have given due consideration to the protection of intellectual property associated with this work and that there are no impediments to publication, including the timing of publication, with respect to intellectual property. In so doing we confirm that we have followed the regulations of our institutions concerning intellectual property.

We further confirm that any aspect of the work covered in this manuscript that has involved human patients has been conducted with the ethical approval of all relevant bodies and that such approvals are acknowledged within the manuscript.

References

[1]. Critchley HD, Corfield DR, Chandler MP, Mathias CJ, Dolan RJ. Cerebral correlates of autonomic cardiovascular arousal: a functional neuroimaging investigation in humans. J Physiol 2000;523(Pt 1):259–70. [PubMed: 10673560]

[2]. Akiki TJ, Averill CL, Abdallah CG. A network-based neurobiological model of PTSD: evidence from structural and functional neuroimaging studies. Curr Psychiatr Rep 2017;19(11):81.

[3]. Merz CJ, Elzinga BM, Schwabe L. Stress, fear, and memory in healthy individuals. Posttraumatic Stress Disorder John Wiley & Sons, Inc; 2016. p. 159–78.

[4]. Anda RF, Brown DW, Felitti VJ, Bremner JD, Dube SR, Giles WH. Adverse childhood experiences and prescribed psychotropic medications in adults. Am J Prev Med 2007;32(5):389–94. [PubMed: 17478264]

[5]. Gurel NZ, Huang M, Wittbrodt MT, Jung H, Ladd SL, Shandhi MMH, et al. Quantifying acute physiological biomarkers of transcutaneous cervical vagal nerve stimulation in the context of psychological stress. Brain Stimul 2020;13(1):47–59. [PubMed: 31439323]

[6]. Pitman RK, Rasmusson AM, Koenen KC, Shin LM, Orr SP, Gilbertson MW, et al. Biological studies of post-traumatic stress disorder. Nat Rev Neurosci 2012;13(11):769–87. [PubMed: 23047775]

[7]. Lupien SJ, McEwen BS, Gunnar MR, Heim C. Effects of stress throughout the lifespan on the brain, behaviour and cognition. Nat Rev Neurosci 2009;10(6): 434–45. [PubMed: 19401723]

[8]. Bremner JD, Randall P, Vermetten E, Staib L, Bronen RA, Mazure C, et al. Magnetic resonance imaging-based measurement of hippocampal volume in posttraumatic stress disorder related to childhood physical and sexual abuse–a preliminary report. Biol Psychiatr 1997;41(1):23–32.

[9]. Lerman I, Davis B, Huang M, Huang C, Sorkin L, Proudfoot J, et al. Noninvasive vagus nerve stimulation alters neural response and physiological autonomic tone to noxious thermal challenge. PloS One 2019;14(2):e0201212. [PubMed: 30759089]

[10]. Lerman I, Hauger R, Sorkin L, Proudfoot J, Davis B, Huang A, et al. Noninvasive transcutaneous vagus nerve stimulation decreases whole blood culture-derived cytokines and chemokines: a randomized, blinded, healthy control pilot trial. Neuromodulation: Technol. Neural Inter 2016;19(3):283–90.

[11]. Zhou L, Lin J, Lin J, Kui G, Zhang J, Yu Y. Neuroprotective effects of vagus nerve stimulation on traumatic brain injury. Neural Regen Res 2014;9(17): 1585–91. [PubMed: 25368644]

[12]. George MS, Rush AJ, Marangell LB, Sackeim HA, Brannan SK, Davis SM, et al. A one-year comparison of vagus nerve stimulation with treatment as usual for treatment-resistant depression. Biol Psychiatr 2005;58(5):364–73.

[13]. Sackeim HA, Brannan SK, Rush AJ, George MS, Marangell LB, Allen J. Durability of antidepressant response to vagus nerve stimulation (VNS). Int J Neuropsychopharmacol 2007;10(6):817–26. [PubMed: 17288644]

[14]. Rong P, Liu J, Wang L, Liu R, Fang J, Zhao J, et al. Effect of transcutaneous auricular vagus nerve stimulation on major depressive disorder: a nonrandomized controlled pilot study. J Affect Disord 2016;195:172–9. [PubMed: 26896810]

[15]. Fang J, Rong P, Hong Y, Fan Y, Liu J, Wang H, et al. Transcutaneous vagus nerve stimulation modulates default mode network in major depressive disorder. Biol Psychiatr 2016;79(4):266–73.

[16]. Pruitt DT, Schmid AN, Kim LJ, Abe CM, Trieu JL, Choua C, et al. Vagus nerve stimulation delivered with motor training enhances recovery of function after traumatic brain injury. J Neurotrauma 2016;33(9):871–9. [PubMed: 26058501]

[17]. Smith DC, Modglin AA, Roosevelt RW, Neese SL, Jensen RA, Browning RA, et al. Electrical stimulation of the vagus nerve enhances cognitive and motor recovery following moderate fluid percussion injury in the rat. J Neurotrauma 2005;22(12):1485–502. [PubMed: 16379585]

[18]. Noble LJ, Meruva VB, Hays SA, Rennaker RL, Kilgard MP, McIntyre CK. Vagus nerve stimulation promotes generalization of conditioned fear extinction and reduces anxiety in rats. Brain Stimul 2019;12(1):9–18. [PubMed: 30287193]

[19]. Clark KB, Krahl SE, Smith DC, Jensen RA. Post-training unilateral vagal stimulation enhances retention performance in the rat. Neurobiol Learn Mem 1995;63(3):213–6. [PubMed: 7670833]

[20]. Clark KB, Smith DC, Hassert DL, Browning RA, Naritoku DK, Jensen RA. Posttraining electrical stimulation of vagal afferents with concomitant vagal efferent inactivation enhances memory storage processes in the rat. Neurobiol Learn Mem 1998;70(3):364–73. [PubMed: 9774527]

[21]. Bansal V, Ryu SY, Lopez N, Allexan S, Krzyzaniak M, Eliceiri B, et al. Vagal stimulation modulates inflammation through a ghrelin mediated mechanism in traumatic brain injury. Inflammation 2012;35(1):214–20. [PubMed: 21360048]

[22]. Lamb DG, Porges EC, Lewis GF, Williamson JB. Non-invasive vagal nerve stimulation effects on hyperarousal and autonomic state in patients with posttraumatic stress disorder and history of mild traumatic brain injury: preliminary evidence. Front Med (Lausanne) 2017;4:124. [PubMed: 28824913]

[23]. Borovikova LV, Ivanova S, Zhang M, Yang H, Botchkina GI, Watkins LR, et al. Vagus nerve stimulation attenuates the systemic inflammatory response to endotoxin. Nature 2000;405(6785):458–62. [PubMed: 10839541]

[24]. Noble LJ, Souza RR, McIntyre CK. Vagus nerve stimulation as a tool for enhancing extinction in exposure-based therapies. Psychopharmacology 2019;236(1):355–67. [PubMed: 30091004]

[25]. Manta S, Dong J, Debonnel G, Blier P. Enhancement of the function of rat serotonin and norepinephrine neurons by sustained vagus nerve stimulation. J Psychiatry Neurosci 2009;34(4):272–80. [PubMed: 19568478]

[26]. Manta S, El Mansari M, Debonnel G, Blier P. Electrophysiological and neurochemical effects of long-term vagus nerve stimulation on the rat monoaminergic systems. Int J Neuropsychopharmacol 2013;16(2):459–70. [PubMed: 22717062]

[27]. Groves DA, Bowman EM, Brown VJ. Recordings from the rat locus coeruleus during acute vagal nerve stimulation in the anaesthetised rat. Neurosci Lett 2005;379(3):174–9. [PubMed: 15843058]

[28]. Kraus T, Hosl K, Kiess O, Schanze A, Kornhuber J, Forster C. BOLD fMRI deactivation of limbic and temporal brain structures and mood enhancing effect by transcutaneous vagus nerve stimulation. J Neural Transm (Vienna) 2007;114(11):1485–93. [PubMed: 17564758]

[29]. Morilak DA, Barrera G, Echevarria DJ, Garcia AS, Hernandez A, Ma S, et al. Role of brain norepinephrine in the behavioral response to stress. Prog Neuro-Psychopharmacol Biol Psychiatry 2005;29(8):1214–24.

[30]. Krahl SE, Clark KB, Smith DC, Browning RA. Locus coeruleus lesions suppress the seizure-attenuating effects of vagus nerve stimulation. Epilepsia 1998;39(7):709–14. [PubMed: 9670898]

[31]. Lerman I, Hauger R, Sorkin L, Proudfoot J, Davis B, Huang A, et al. Noninvasive transcutaneous vagus nerve stimulation decreases whole blood culture-derived cytokines and chemokines: a

randomized, blinded, healthy control pilot trial. Neuromodulation 2016;19(3):283–90. [PubMed: 26990318]

[32]. Clark KB, Naritoku DK, Smith DC, Browning RA, Jensen RA. Enhanced recognition memory following vagus nerve stimulation in human subjects. Nat Neurosci 1999;2(1):94–8. [PubMed: 10195186]

[33]. Sackeim HA, Keilp JG, Rush AJ, George MS, Marangell LB, Dormer JS, et al. The effects of vagus nerve stimulation on cognitive performance in patients with treatment-resistant depression. Neuropsys. Neuropsychol. Behav Neuro 2001;14:53–62.

[34]. Suthana N, Fried I. Deep brain stimulation for enhancement of learning and memory. Neuroimage 2014;85:996–1002. [PubMed: 23921099]

[35]. Lewine JD, Paulson K, Bangera N, Simon BJ. Exploration of the impact of brief noninvasive vagal nerve stimulation on EEG and event-related potentials. Neuromodulation 2018;22(5):564–72. 10.1111/ner.12864. [PubMed: 30288866]

[36]. Bremner JD, Rapaport MH. Vagus nerve stimulation: back to the future. Am J Psychiatr 2017;174(7):609–10. [PubMed: 28669203]

[37]. Neren D, Johnson MD, Legon W, Bachour SP, Ling G, Divani AA. Vagus nerve stimulation and other neuromodulation methods for treatment of traumatic brain injury. Neurocritical Care 2016;24(2):308–19. [PubMed: 26399249]

[38]. Mourdoukoutas AP, Truong DQ, Adair DK, Simon BJ, Bikson M. High-resolution multi-scale computational model for non-invasive cervical vagus nerve stimulation. Neuromodulation 2018;21(3):261–8. [PubMed: 29076212]

[39]. Nonis R, D'Ostilio K, Schoenen J, Magis D. Evidence of activation of vagal afferents by non-invasive vagus nerve stimulation: an electrophysiological study in healthy volunteers. Cephalalgia 2017;37(13):1285–93. [PubMed: 28648089]

[40]. Usami K, Kawai K, Sonoo M, Saito N. Scalp-recorded evoked potentials as a marker for afferent nerve impulse in clinical vagus nerve stimulation. Brain Stimul 2013;6(4):615–23. [PubMed: 23088852]

[41]. Frangos E, Komisaruk BR. Access to vagal projections via cutaneous electrixal stimulation of the neck: fMRI evidence in healthy humans. Brain Stimulation 2017;10:19–27. [PubMed: 28104084]

[42]. Frangos E, Ellrich E, Komisaruk BR. Non-invasive access to the vagus nerve central projections via electrical stimulation of the external ear: fMRI evidence in humans. Brain Stimulation 2015;8:624–36. [PubMed: 25573069]

[43]. Yakunina N, Kim SS, Nam EC. Optimization of transcutaneous vagus nerve stimulation using functional MRI. Neuromodulation 2017;20(3):290–300. [PubMed: 27898202]

[44]. Badran BW, Dowdle LT, Mithoefer OJ, LaBate NT, Coatsworth J, Brown JC, et al. Neurophysiologic effects of transcutaneous auricular vagus nerve stimulation (taVNS) via electrical stimulation of the tragus: a concurrent taVNS/fMRI study and review. Brain Stimul 2018;11(3):492–500. [PubMed: 29361441]

[45]. Bremner JD, Narayan M, Staib LH, Southwick SM, McGlashan T, Charney DS. Neural correlates of memories of childhood sexual abuse in women with and without posttraumatic stress disorder. Am J Psychiatr 1999;156(11): 1787–95. [PubMed: 10553744]

[46]. Liberzon I, Britton JC, Phan KL. Neural correlates of traumatic recall in posttraumatic stress disorder. Stress 2003;6(3):151–6. [PubMed: 13129808]

[47]. Lanius RA, Williamson PC, Densmore M, Boksman K, Gupta MA, Neufeld RW, et al. Neural correlates of traumatic memories in posttraumatic stress disorder: a functional MRI investigation. Am J Psychiatr 2001;158(11):1920–2. [PubMed: 11691703]

[48]. Lindauer RJ, Booij J, Habraken JB, van Meijel EP, Uylings HB, Olff M, et al. Effects of psychotherapy on regional cerebral blood flow during trauma imagery in patients with post-traumatic stress disorder: a randomized clinical trial. Psychol Med 2008;38(4):543–54. [PubMed: 17803835]

[49]. Etkin A, Wager T. Functional neuroimaging of anxiety: a meta-analysis of emotional processing in PTSD, social anxiety disorder, and specific phobia. Am J Psychiatr 2007;164(10).

[50]. American Psychiatric Association. In: The diagnostic and statistical manual of mental disorders. fifth ed. Washington, D.C.: American Psychiatric Association; 2013 (DSM-5). 5 ed.

[51]. Weathers FW, Bovin MJ, Lee DJ, Sloan DM, Schnurr PP, Kaloupek DG, et al. The Clinician-Administered PTSD Scale for DSM-5 (CAPS-5): development and initial psychometric evaluation in military veterans. Psychol Assess 2018;30(3):383–95. [PubMed: 28493729]

[52]. Bremner JD, Bolus R, Mayer EA. Psychometric properties of the early trauma inventory-self report. J Nerv Ment Dis 2007;195(3):211–8. [PubMed: 17468680]

[53]. Bremner JD, Vermetten E, Mazure CM. Development and preliminary psychometric properties of an instrument for the measurement of childhood trauma: the Early Trauma Inventory. Depress Anxiety 2000;12(1):1–12. [PubMed: 10999240]

[54]. Wittbrodt MT, Vaccarino V, Shah AJ, Mayer EA, Bremner JD. Psychometric properties of the adulthood trauma inventory. Health Psychol 2020. 10.1037/hea0000856. In press.

[55]. First MB, Gibbon M. The structured clinical interview for DSM-IV Axis I disorders (SCID-I) and the structured clinical interview for DSM-IV Axis II disorders (SCID-II). In: Segal MJHDL, editor Comprehensive handbook of psychological assessment. Hoboken, NJ, US: John Wiley & Sons Inc.; 2004. p. 134–43.

[56]. Schmand M, Wienhard K, Casey M, Eriksson L, Jones W, Reed J, et al. Performance evaluation of a new LSO high resolution research tomograph-HRRT. In: Nuclear science symposium, 1999. Conference record. 1999 IEEE, vol. 2. IEEE; 1999. p. 1067–71.

[57]. Bremner JD, Campanella C, Khan Z, Shah M, Hammadah M, Wilmot K, et al. Brain correlates of mental stress-induced myocardial ischemia. Psychosom Med 2018;80(6):515–25. 10.1097/PSY.0000000000000597. [PubMed: 29794945]

[58]. Gläscher J, Gitelman D. Contrast weights in flexible factorial design with multiple groups of subjects. Sml. SPM@ JISCMAIL AC UK; 2008. p. 1–12.

[59]. Lane RD, Reiman EM, Ahern GL, Schwartz GE, Davidson RJ. Neuroanatomical correlates of happiness, sadness, and disgust. Am J Psychiatr 1997;154(7): 926–33. [PubMed: 9210742]

[60]. Reiman EM, Lane RD, Ahern GL, Schwartz GE, Davidson RJ, Friston KJ, et al. Neuroanatomical correlates of externally and internally generated human emotion. Am J Psychiatr 1997;154(7):918–25. [PubMed: 9210741]

[61]. Talairach J, Tournoux P. Co-planar stereotaxic atlas of the human brain: 3-dimensional proportional system: an approach to cerebral imaging. 1988.

[62]. Lanius RA, Williamson PC, Densmore M, Boksman K, Neufeld RW, Gati JS, et al. The nature of traumatic memories: a 4-T FMRI functional connectivity analysis. Am J Psychiatr 2004;161(1):36–44. [PubMed: 14702248]

[63]. Bremner JD, Staib LH, Kaloupek D, Southwick SM, Soufer R, Charney DS. Neural correlates of exposure to traumatic pictures and sound in Vietnam combat veterans with and without posttraumatic stress disorder: a positron emission tomography study. Biol Psychiatr 1999;45(7):806–16.

[64]. Bremner JD, Vythilingam M, Vermetten E, Southwick SM, McGlashan T, Nazeer A, et al. MRI and PET study of deficits in hippocampal structure and function in women with childhood sexual abuse and posttraumatic stress disorder (PTSD). Am J Psychiatr 2003;160(5):924–32. [PubMed: 12727697]

[65]. Britton JC, Phan KL, Taylor SF, Fig LM, Liberzon I. Corticolimbic blood flow in posttraumatic stress disorder during script-driven imagery. Biol Psychiatr 2005;57(8):832–40.

[66]. Bremner JD, Narayan M, Staib LH, Southwick SM, McGlashan T, Charney DS. Neural correlates of memories of childhood sexual abuse in women with and without posttraumatic stress disorder. Am J Psychiatr 1999;156(11): 1787–95. [PubMed: 10553744]

[67]. Rauch SL, van der Kolk BA, Fisler RE, Alpert NM, Orr SP, Savage CR, et al. A symptom provocation study of posttraumatic stress disorder using positron emission tomography and script-driven imagery. Arch Gen Psychiatr 1996;53(5):380–7. [PubMed: 8624181]

[68]. Osuch EA, Benson B, Geraci M, Podell D, Herscovitch P, McCann UD, et al. Regional cerebral blood flow correlated with flashback intensity in patients with posttraumatic stress disorder. Biol Psychiatr 2001;50(4):246–53.

[69]. Dixon ML, Thiruchselvam R, Todd R, Christoff K. Emotion and the prefrontal cortex: an integrative review. Psychol Bull 2017;143(10):1033–81. [PubMed: 28616997]

[70]. Gilboa A, Shalev AY, Laor L, Lester H, Louzoun Y, Chisin R, et al. Functional connectivity of the prefrontal cortex and the amygdala in posttraumatic stress disorder. Biol Psychiatr 2004;55(3):263–72.

[71]. Lindquist KA, Satpute AB, Wager TD, Weber J, Barrett LF. The brain basis of positive and negative affect: evidence from a meta-analysis of the human neuroimaging literature. Cerebr Cortex 2016;26(5):1910–22.

[72]. Kross E, Davidson M, Weber J, Ochsner K. Coping with emotions past: the neural bases of regulating affect associated with negative autobiographical memories. Biol Psychiatr 2009;65(5):361–6.

[73]. Devinsky O, Morrell MJ, Vogt BA. Contributions of anterior cingulate cortex to behaviour. Brain 1995;118(Pt 1):279–306. [PubMed: 7895011]

[74]. Bush G, Luu P, Posner MI. Cognitive and emotional influences in anterior cingulate cortex. Trends Cognit Sci 2000;4(6):215–22. [PubMed: 10827444]

[75]. Kraynak TE, Marsland AL, Gianaros PJ. Neural mechanisms linking emotion with cardiovascular disease. Curr Cardiol Rep 2018;20(12):128. [PubMed: 30311094]

[76]. Hays SA, Rennaker RL, Kilgard MP. Targeting plasticity with vagus nerve stimulation to treat neurological disease. Prog Brain Res 2013;207:275–99. [PubMed: 24309259]

[77]. Detari L, Juhasz G, Kukorelli T. Effect of stimulation of vagal and radial nerves on neuronal activity in the basal forebrain area of anaesthetized cats. Acta Physiol Hung 1983;61(3):147–54. [PubMed: 6650184]

[78]. Follesa P, Biggio F, Gorini G, Caria S, Talani G, Dazzi L, et al. Vagus nerve stimulation increases norepinephrine concentration and the gene expression of BDNF and bFGF in the rat brain. Brain Res 2007;1179:28–34. [PubMed: 17920573]

[79]. Gurel NZ, Wittbrodt MT, Jung H, Ladd SL, Shah AJ, Vaccarino V, et al. Automatic detection of target engagement in transcutaneous cervical vagal nerve stimulation for traumatic stress triggers. IEEE J Biomed Health Inform 2020;24(7):1917–25. 10.1109/JBHI.2020.2981116. [PubMed: 32175881]

[80]. Gurel NZ, Gazi AH, Scott KL, Wittbrodt MT, Shah AJ, Vaccarino V, et al. Timing considerations for noninvasive vagal nerve stimulation in clinical studies. AMIA Annu Symp Proc 2019;2019:1061–70. [PubMed: 32308903]

[81]. Shetake JA, Engineer ND, Vrana WA, Wolf JT, Kilgard MP. Pairing tone trains with vagus nerve stimulation induces temporal plasticity in auditory cortex. Exp Neurol 2012;233(1):342–9. [PubMed: 22079155]

[82]. Weiner KS, Zilles K. The anatomical and functional specialization of the fusiform gyrus. Neuropsychologia 2016;83:48–62. [PubMed: 26119921]

[83]. Goodale MA, Milner AD. Separate visual pathways for perception and action. Trends Neurosci 1992;15:20–5. [PubMed: 1374953]

[84]. Silson EH, Gilmore AW, Kalinowski SE, Steel A, Kidder A, Martin A, et al. A posterior-anterior distinction between scene perception and scene construction in human medial parietal cortex. J Neurosci 2019;39(4):705–17. [PubMed: 30504281]

[85]. Svoboda E, McKinnon MC, Levine B. The functional neuroanatomy of autobiographical memory: a meta-analysis. Neuropsychologia 2006;44(12): 2189–208. [PubMed: 16806314]

[86]. Kulkarni B, Bentley DE, Elliott R, Youell P, Watson A, Derbyshire SW, et al. Attention to pain localization and unpleasantness discriminates the functions of the medial and lateral pain systems. Eur J Neurosci 2005;21(11): 3133–42. [PubMed: 15978022]

[87]. Goldin PR, McRae K, Ramel W, Gross JJ. The neural bases of emotion regulation: reappraisal and suppression of negative emotion. Biol Psychiatr 2008;63(6):577–86.

[88]. Noble IJ, Gonzalez IJ, Meruva VB, Callahan KA, Belfort BD, Ramanathan KR, et al. Effects of vagus nerve stimulation on extinction of conditioned fear and post-traumatic stress disorder symptoms in rats. Transl Psychiatry 2017;7(e1217):1–8.

[89]. Souza RR, Robertson NM, Pruitt DT, Gonzales PA, Hays SA, Rennaker RL, et al. Vagus nerve stimulation reverses the extinction impairments in a model of PTSD with prolonged and repeated trauma. Stress 2019;22(4):509–20. [PubMed: 31010369]

[90]. Burger AM, Van der Does W, Thayer JF, Brosschot JF, Verkuil B. Transcutaneous vagus nerve stimulation reduces spontaneous but not induced negative thought intrusions in high worriers. Biol Psychol 2019;142:80–9. [PubMed: 30710565]

[91]. Burger AM, Verkuil B, Fenlon H, Thijs L, Cools L, Miller HC, et al. Mixed evidence for the potential of non-invasive transcutaneous vagal nerve stimulation to improve the extinction and retention of fear. Behav Res Ther 2017;97:64–74. [PubMed: 28719827]

[92]. Burger AM, Verkuil B, Van Diest I, Van der Does W, Thayer JF, Brosschot JF. The effects of transcutaneous vagus nerve stimulation on conditioned fear extinction in humans. Neurobiol Learn Mem 2016;132:49–56. [PubMed: 27222436]

[93]. Burger AM, Van Diest I, van der Does W, Hysaj M, Thayer JF, Brosschot JF, et al. Transcutaneous vagus nerve stimulation and extinction of prepared fear: a conceptual non-replication. Sci Rep 2018;8(1):11471. [PubMed: 30065275]

[94]. Bremner JD, Mishra S, Campanella C, Shah M, Kasher N, Evans S, et al. A pilot study of the effects of mindfulness-based stress reduction on post-traumatic stress disorder symptoms and brain response to traumatic reminders of combat in operation enduring freedom/operation Iraqi freedom combat veterans with post-traumatic stress disorder. Front Psychiatr 2017;8:157.

[95]. Campanella C, Bremner JD. Neuroimaging of PTSD. In: Bremner JD, editor. Posttraumatic stress disorder: from neurobiology to treatment. Hoboken, New Jersey: Wiley-Blackwell; 2016. p. 291–320.

[96]. Cain C, Sullivan R. Amygdala contributions to fear and safety conditioning: insights into PTSD from an animal model across development. Posttraumatic Stress Disorder: From Neurobiology to Treatment 2016:81–104.

[97]. Zoladz PR, Diamond D. Psychosocial predator stress model of PTSD based on clinically relevant risk factors for trauma-induced psychopathology. Posttraumatic Stress Disorder: From Neurobiology to Treatment 2016;125: 125–43.

[98]. Kraus T, Kiess O, Hosl K, Terekhin P, Kornhuber J, Forster C. CNS BOLD fMRI effects of sham-controlled transcutaneous electrical nerve stimulation in the left outer auditory canal - a pilot study. Brain Stimul 2013;6(5):798–804. [PubMed: 23453934]

[99]. Fallgatter AJ, Neuhauser B, Herrmann MJ, Ehlis A-C, Wagener A, Scheuerpflug P, et al. Far field potentials from the brain stem after transcutaneous vagus nerve stimulation. J Neural Transm 2003;110:1437–43. [PubMed: 14666414]

[100]. Polak T, Markulin F, Ehlis A-C, Langer JBM, Ringel TM, Fallgatter AJ. Far field potentials from brain stem after transcutaneous vagus nerve stimulation: optimization of stimulation and recording parameters. J Neural Transm 2009;116:1237–42. [PubMed: 19728032]

[101]. Dimitrov B, Gatev P. Effects of acute transcutaneous vagal stimulation on the EEG power maps, EEG sources distribution and steadiness of quiet and sensory-conflicted stance. Balance Brain: Int Works Proc. 2015:45–54.

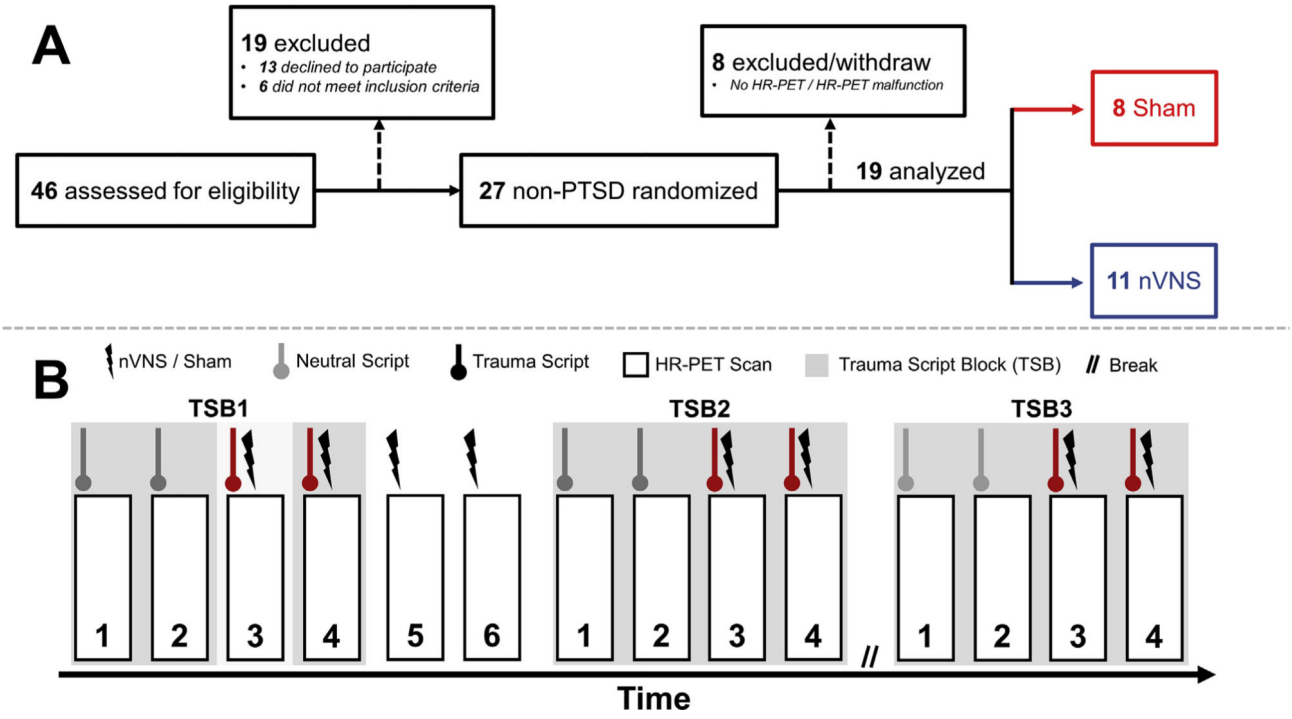

Fig. 1.

Participant recruitment and study timeline. A: Consolidated Standards of Reporting Trials (CONSORT) diagram of the study. HR-PET = High Resolution Positron Emission Tomography; nVNS = non-invasive vagal nerve stimulation. B: Protocol timeline for the High-Resolution Positron Emission Tomography (HR-PET) scanning session. All trauma scripts were delivered via headphones with non-invasive cervical vagal nerve stimulation (nVNS) or sham stimulation occurring after script completion. Total scanning session length was 5 h, with each trauma script/HR-PET scan lasting 2 min and stimulation lasting 2 min. The rest period lasted for 90 min and time between scans was approximately 5 min.

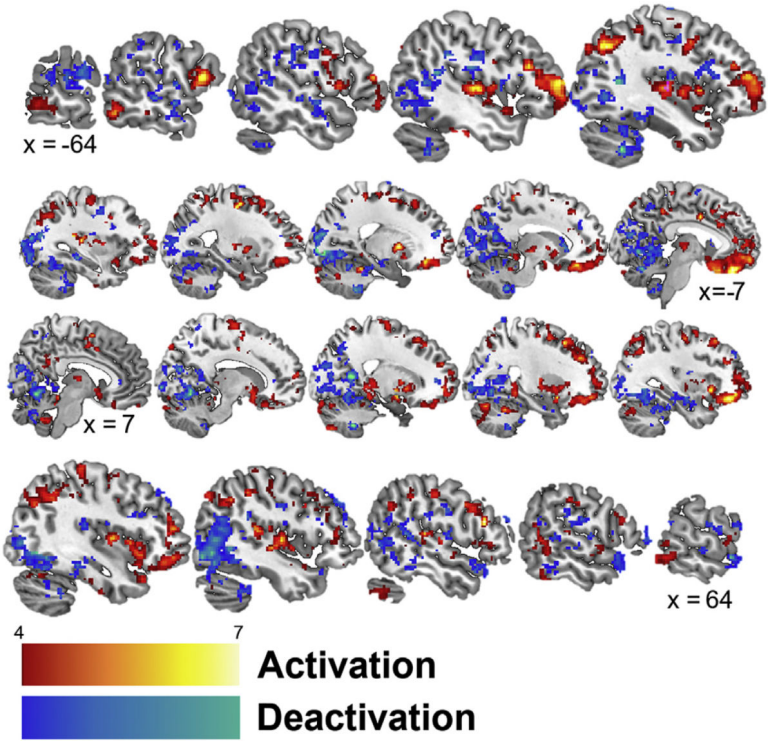

Fig. 2.

Sagittal slices presenting significant ($p < 0.005$) activation (red) and deactivation (blue) while listening to personalized trauma scripts in participants receiving cervical non-invasive vagal nerve and sham stimulation. Talairach x coordinates below slices indicate location with negative and positive coordinates located in the left and right hemisphere, respectively. Color bars indicate z-values of cluster.

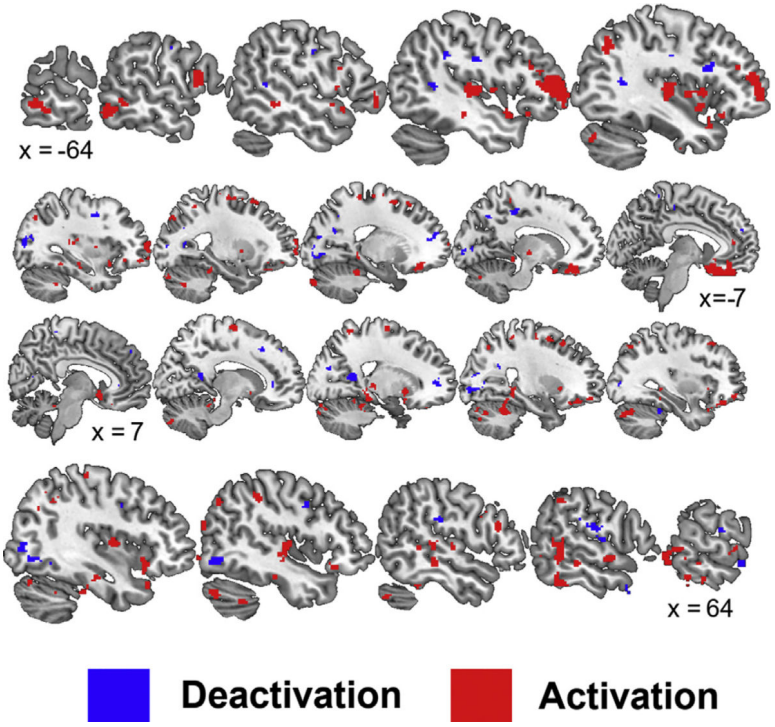

Fig. 3.

Sagittal slices presenting significant ($p < 0.005$) areas with greater activation (red) and deactivation (blue) while listening to personalized traumatic scripts and application of a sham compared to non-invasive cervical vagal nerve stimulation (nVNS). Talairach x coordinates below slices indicate location with negative and positive coordinates located in the left and right hemisphere, respectively.

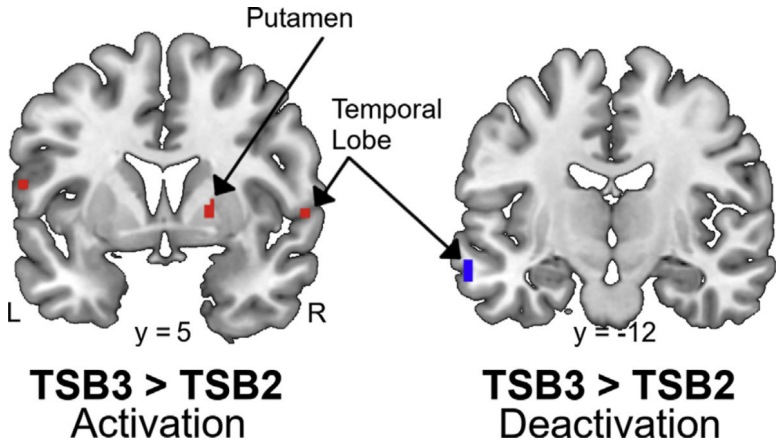

Fig. 4.

Coronal slices of significant ($p < 0.0025$) areas with greater activation (red) and deactivation (blue) during the third compared to second personalized trauma script block (TSB). Color gradient indicates magnitude of activation/deactivation. Talairach y coordinates below slices indicate location with negative and positive coordinates located in the left and right hemisphere, respectively.

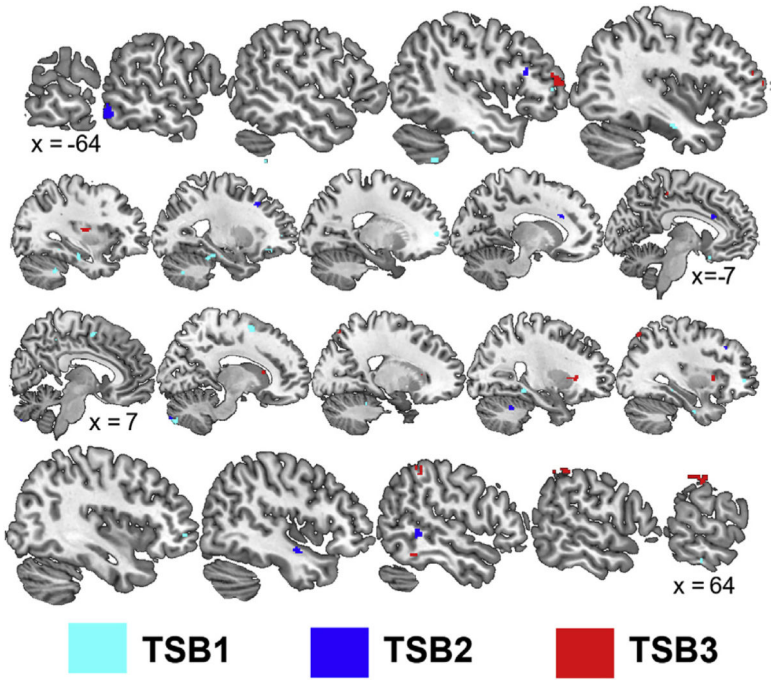

Fig. 5.

Sagittal slices presenting significant ($p < 0.0017$) areas with greater activation during the trauma scripts in participants receiving sham compared to non-invasive cervical vagal nerve stimulation (nVNS) during the first (TSB1), second (TSB2), and third (TSB3) iterations of trauma exposure. Talairach x coordinates below slices indicate location with negative and positive coordinates located in the left and right hemisphere, respectively.

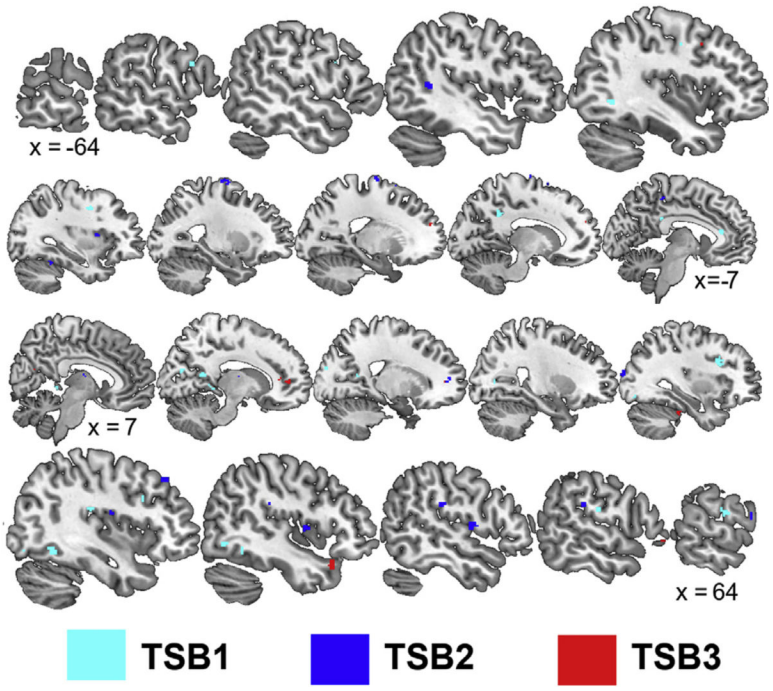

Fig. 6.

Sagittal slices presenting significant ($p < 0.0017$) areas with greater deactivation during the trauma scripts in participants receiving sham compared to non-invasive cervical vagal nerve stimulation (nVNS) during the first (TSB1), second (TSB2), and third (TSB3) iterations of trauma exposure. Talairach x coordinates below slices indicate location with negative and positive coordinates located in the left and right hemisphere, respectively.

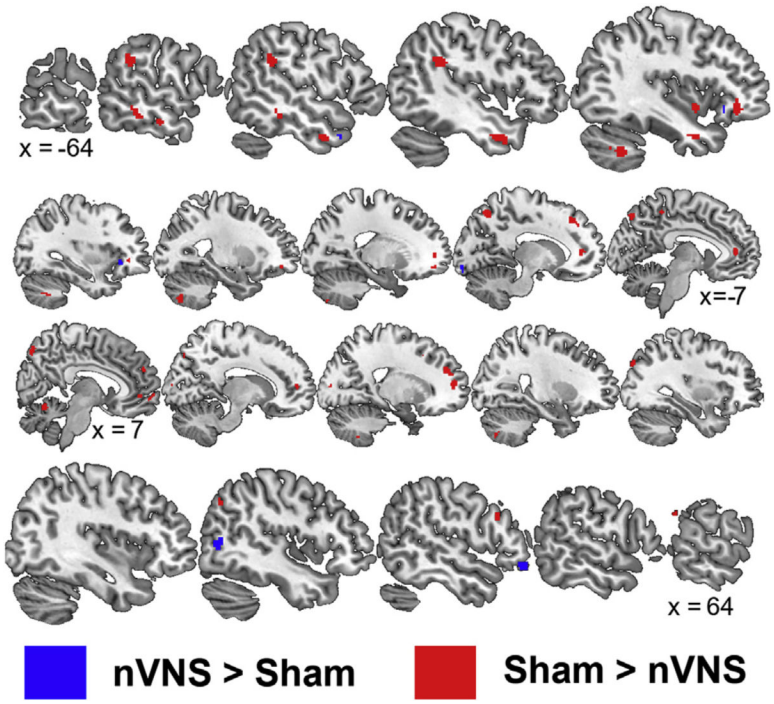

Fig. 7.

Sagittal slices presenting significant ($p < 0.005$) areas with greater activation (red) during sham compared to non-invasive cervical vagal nerve stimulation (nVNS) and during nVNS compared to sham (blue) during resting conditions. Talairach x coordinates below slices indicate location with negative and positive coordinates located in the left and right hemisphere, respectively.

Table 1

Participant Demographics for the active non-invasive vagal nerve stimulation (nVNS) and sham groups.

Measure	nVNS (n = 11)	Sham (n = 8)	p value
Age (y)	28.7 ± 8.4	25.3 ± 3.4	0.90
Sex	4 F, 7 M	5 F, 3 M	0.37
BMI (kg·m^{-2}),	26.2 ± 5.7	28.5 ± 5.3	0.38
PTSD Checklist Score	29.3 ± 9.5	29.4 ± 10.3	0.65
Early Trauma Inventory	11.0 ± 7.1	8.8 ± 6.9	0.53
Adulthood Trauma Inventory	4.1 ± 1.6	3.5 ± 2.9	0.68
Race/Ethnicity			0.14
White/Caucasian	5 (45.5%)	1 (12.5%)	
Black/African American	3 (27.3%)	2 (25.0%)	
Asian	1 (9.1%)	4 (50.0%)	
Multiracial	–	1 (12.5%)	
Other	2 (18.2%)	–	
Marital Status			1.0
Never Married	8 (72.7%)	7 (87.5%)	
Married/Civil Partnership	2 (18.2%)	1 (14.3%)	
Divorced/Separated	1 (9.1%)	–	

Table 2

Brain areas with significantly ($p < 0.005$) greater activations in participants receiving sham compared with non-invasive cervical vagal nerve (nVNS) stimulation during exposure to personalized trauma scripts as measured with positron emission tomography. Significant clusters are presented by size (number of voxels) and location (Brodmann area, cluster peak Talairach coordinates). Sub-cluster peaks are also identified.

Voxel Number	Brain Region	Brodmann Area	Talairach			Z Score
			X	Y	Z	
594	L Frontal Lobe, Middle Gyrus	10	−44	51	6	4.98
	L Frontal Lobe, Inferior Gyrus	46	−44	43	8	4.62
	L Frontal Lobe, Superior Gyrus	10	−30	62	0	3.74
19	L Frontal Lobe, Inferior Gyrus	45	−48	26	17	4.40
37	R Temporal Lobe, Superior Gyrus	42	67	−21	13	4.35
36	R Frontal Lobe, Inferior Gyrus	45	51	24	16	4.35
339	R Parahippocampal Gyrus	36	22	−37	−5	4.16
	R Parahippocampal Gyrus	35	18	−32	−10	3.91
	R Cerebellum		26	−50	−21	3.79
177	L Claustrum		−38	−15	6	4.14
	L Temporal Lobe, Superior Gyrus	22	−46	−17	6	3.99
60	R Frontal Lobe, Middle Gyrus	8	26	20	41	4.07
	R Frontal Lobe, Middle Gyrus	8	32	27	41	3.22
121	R Claustrum		38	−4	5	4.02
	R Temporal Lobe, Superior Gyrus	22	46	−18	−1	3.70
	R Temporal Lobe, Superior Gyrus	22	51	−12	2	3.47
58	L Cerebellum		−20	−38	−18	4.02
75	L Anterior Cingulate Gyrus	32	−2	25	29	4.01
921	L Frontal Lobe, Inferior Gyrus	11	−14	34	−17	3.99
	L Frontal Lobe, Rectal Gyrus	11	−6	38	−22	3.98
	L Frontal Lobe, Rectal Gyrus	11	−6	22	−21	3.83
12	L Parahippocampal Gyrus		−34	−20	−11	3.86
97	L Insula	13	−42	8	1	3.69
	L Claustrum		−38	−2	2	3.56
	L Frontal Lobe, Precentral Gyrus	6	−48	−2	5	3.12

Voxel Number	Brain Region	Brodmann Area	Talairach			Z Score
			X	Y	Z	
69	R Frontal Lobe, Inferior Gyrus	47	42	21	−9	3.62
23	L Anterior Cingulate	32	−8	41	8	3.62
38	R Parietal Lobe, Inferior Lobule	40	48	−35	37	3.61
103	R Temporal Lobe, Fusiform Gyrus	20	55	−42	−21	3.58
	R Temporal Lobe, Inferior Gyrus	20	61	−42	−16	3.04
47	R Frontal Lobe, Middle Gyrus	11	30	48	−12	3.57
254	R Temporal Lobe, Middle Gyrus	21	59	−43	−3	3.55
	R Temporal Lobe, Middle Gyrus	21	61	−54	3	3.53
	R Temporal Lobe, Middle Gyrus	22	55	−41	4	3.33
120	L Frontal Lobe, Precentral Gyrus	44	−59	10	13	3.53
	L Frontal Lobe, Precentral Gyrus	44	−55	10	6	3.18
	L Temporal Lobe, Superior Gyrus	22	−61	2	5	3.00
106	R Frontal Lobe, Medial Gyrus	6	14	−5	57	3.53
	R Frontal Lobe, Precentral Gyrus	6	28	−9	49	2.84
31	L Thalamus		−12	−16	−1	3.52
105	L Insula	13	−42	5	−7	3.49
	L Frontal Lobe, Inferior Gyrus	13	−32	13	−11	3.27
	L Temporal Lobe, Superior Gyrus	38	−40	13	−19	3.01
32	L Parietal Lobe, Postcentral Gyrus	3	−18	−32	54	3.44
154	L Temporal Lobe, Middle Gyrus	21	−65	−45	−3	3.39
	L Temporal Lobe, Inferior Gyrus	37	−57	−55	−7	3.19
	L Temporal Lobe, Middle Gyrus	21	−55	−47	−1	2.98
27	L Cerebellum		−24	−62	−31	3.39
	L Cerebellum		−24	−69	−27	2.89
12	L Cerebellum		−32	−46	−28	3.38
23	L Insula	13	−32	−25	10	3.38
	L Insula	13	−36	−21	14	3.14
89	L Frontal Lobe, Middle Gyrus	8	−26	18	49	3.37
	L Frontal Lobe, Superior Gyrus	8	−18	24	46	3.18
	L Frontal Lobe, Middle Gyrus	6	−22	6	47	3.01

Voxel Number	Brain Region	Brodmann Area	Talairach			Z Score
			X	Y	Z	
138	R Frontal Lobe, Middle Gyrus	11	28	36	−15	3.37
	R Temporal Lobe, Superior Gyrus	38	36	20	−24	3.09
	R Frontal Lobe, Inferior Gyrus	47	30	20	−19	2.73
48	L Parietal Lobe, Precuneus	19	−28	−76	37	3.34
	L Parietal Lobe, Precuneus	19	−34	−66	37	2.98
34	R Cerebellum		42	−50	−33	3.32
	R Cerebellum		40	−52	−26	2.75
30	L Parahippocampal Gyrus	30	−16	−35	−5	3.32
	L Parahippocampal Gyrus	27	−18	−37	2	2.76
75	R Temporal Lobe, Superior Gyrus	22	55	−4	−7	3.31
	R Temporal Lobe, Superior Gyrus	22	61	−2	3	3.07
50	R Temporal Lobe, Middle Gyrus	21	55	−29	−7	3.30
54	L Parietal Lobe, Angular Gyrus	39	−40	−58	36	3.29
171	R Cerebellum		30	−69	−22	3.29
	R Cerebellum		32	−77	−23	3.27
	R Cerebellum		20	−79	−16	2.88
48	R Parahippocampal Gyrus	36	42	−22	−17	3.26
32	R Frontal Lobe, Middle Gyrus	6	28	4	47	3.26
36	L Cerebellum		−20	−87	−26	3.25
28	L Frontal Lobe, Inferior Gyrus	47	−42	25	−13	3.25
11	L Parahippocampal Gyrus	37	−34	−41	−8	3.18
16	R Frontal Lobe, Inferior Gyrus	9	50	11	28	3.17
15	R Cerebellum		0	−38	−17	3.15
53	R Parietal Lobe, Angular Gyrus	39	40	−62	33	3.14
11	L Cerebellum		−24	−34	−27	3.13
14	L Temporal Lobe, Superior Gyrus		−69	−23	−2	3.13
17	L Parietal Lobe, Precuneus	7	−24	−50	48	3.09
	L Parietal Lobe, Precuneus	7	−30	−44	51	2.67
13	R Cerebellum		12	−79	−30	3.09
14	L Cerebellum		−18	−69	−22	3.08

Voxel Number	Brain Region	Brodmann Area	Talairach			Z Score
			X	Y	Z	
24	R Temporal Lobe, Transverse Gyrus	41	53	−23	10	3.08
	R Temporal Lobe, Superior Gyrus	41	50	−31	8	2.97
39	R Parietal Lobe, Superior Lobule	7	28	−64	42	3.05
37	R Thalamus		20	−21	−1	3.04
47	L Frontal Lobe, Middle Gyrus	11	−30	48	−11	3.03
14	R Cerebellum		36	−30	−27	3.02
13	R Temporal Lobe, Inferior Gyrus	20	63	−26	−19	3.00
12	R Occipital Lobe, Middle Gyrus	18	44	−85	1	2.99
14	L Temporal Lobe, Inferior Gyrus	20	−48	−26	−10	2.97
15	L Frontal Lobe, Medial Gyrus	11	−2	50	−11	2.97
49	L Frontal Lobe, Precentral Gyrus	6	−22	−17	56	2.96
	L Frontal Lobe, Sub-Gyral	6	−24	−5	52	2.92
	L Frontal Lobe, Middle Gyrus	6	−16	−7	59	2.74
33	L Cerebellum		−38	−75	−23	2.96
24	R Cerebellum		22	−88	−21	2.96
24	L Temporal Lobe, Superior Gyrus	38	−50	13	−9	2.95
	L Temporal Lobe, Superior Gyrus	38	−53	7	−5	2.94
14	R Parietal Lobe, Supramarginal Gyrus	40	40	−49	34	2.93
18	R Temporal Lobe, Middle Gyrus	39	48	−75	22	2.92
24	R Parietal Lobe, Precuneus	7	20	−50	56	2.90
14	R Parietal Lobe, Inferior Lobule	40	34	−54	45	2.89
44	R Cerebellum		48	−69	−27	2.88
15	R Parietal Lobe, Postcentral Gyrus	3	40	−25	53	2.87
12	R Parietal Lobe, Postcentral Gyrus	3	28	−36	50	2.86
15	R Parahippocampal Gyrus	36	34	−35	−10	2.85
	R Temporal Lobe, Fusiform Gyrus	20	36	−42	−15	2.69
16	R Parietal Lobe, Supramarginal Gyrus	40	55	−41	36	2.84
21	L Cerebellum		−28	−83	−19	2.79
13	L Temporal Lobe, Inferior Gyrus	20	−40	−9	−33	2.79

Table 3

Brain areas with significantly($p < 0.005$) greater deactivation in participants receiving sham compared to non-invasive cervical vagal nerve stimulation (nVNS) while listening to personalized traumatic scripts as measured with positron emission tomography. Significant clusters are presented by size (number of voxels) and location (Brodmann area, cluster peak Talairach coordinates). Sub-cluster peaks are also identified.

Voxel Number	Brain Region	Brodmann Area	Talairach			Z Score
			X	Y	Z	
136	R Posterior Cingulate	29	16	−48	11	4.64
	R Occipital Lobe, Precuneus		26	−51	21	2.68
23	R Temporal Lobe, Middle Gyrus	21	63	3	−9	4.49
129	R Temporal Lobe, Transverse Gyrus	42	61	−13	16	4.26
	R Parietal Lobe, Postcentral Gyrus	43	67	−7	15	4.12
	R Temporal Lobe, Superior Gyrus	22	69	−3	9	3.44
99	L Occipital Lobe, Lingual Gyrus	17	−20	−80	2	3.90
	L Occipital Lobe, Cuneus	17	−16	−89	6	3.76
	L Occipital Lobe, Cuneus	17	−12	−79	7	3.40
212	R Occipital Lobe, Inferior Gyrus	19	38	−68	−2	3.69
	R Occipital Lobe, Inferior Gyrus	19	44	−74	−5	3.58
	R Occipital Lobe, Middle Gyrus	37	40	−64	6	3.42
41	R Anterior Cingulate	10	16	47	−1	3.62
51	L Occipital Lobe, Middle Gyrus	19	−34	−83	14	3.56
	L Occipital Lobe, Middle Gyrus		−32	−71	15	3.36
38	L Frontal Lobe, Medial Gyrus	10	−20	49	13	3.55
44	L Posterior Cingulate Gyrus	31	−14	−27	42	3.54
	L Posterior Cingulate Gyrus	31	−8	−23	45	2.98
27	L Frontal Lobe, Precentral Gyrus	6	−32	2	35	3.39
46	L Temporal Lobe, Middle Gyrus		−44	−46	9	3.36
	L Temporal Lobe, Superior Gyrus	22	−40	−52	13	3.26
	L Temporal Lobe, Superior Gyrus	22	−55	−44	11	3.22
12	R Frontal Lobe, Paracentral Lobule	5	4	−32	54	3.35
81	R Occipital Lobe, Middle Gyrus	18	26	−85	2	3.35
	R Occipital Lobe, Cuneus	30	22	−70	8	3.14

Voxel Number	Brain Region	Brodmann Area	Talairach			Z Score
			X	Y	Z	
12	L Frontal Lobe, Paracentral Lobule	5	−4	−40	57	3.31
26	L Frontal Lobe, Precentral Gyrus	6	−44	−14	26	3.31
28	L Frontal Lobe, Middle Frontal Gyrus	46	−40	14	18	3.29
15	R Anterior Cingulate	24	10	35	3	3.28
14	R Cerebellum		30	−36	−22	3.27
19	L Frontal Lobe, Medial Gyrus	9	−2	51	14	3.26
45	R Frontal Lobe, Precentral Gyrus	9	42	4	32	3.25
16	R Posterior Cingulate	30	8	−69	13	3.22
17	L Frontal Lobe, Precentral Gyrus	6	−53	−6	30	3.21
45	R Occipital Lobe, Cuneus	18	24	−77	17	3.21
	R Parietal Lobe, Precuneus	31	18	−73	22	3.14
16	R Anterior Cingulate	32	12	25	36	3.21
13	L Parietal Lobe, Inferior Lobule	40	−46	−37	29	3.16
24	L Occipital Lobe, Precuneus	31	−20	−63	25	3.16
	L Temporal Lobe, Middle Gyrus	39	−28	−63	27	2.78
12	L Parietal Lobe, Precuneus	7	−14	−58	36	3.14
11	L Posterior Cingulate	30	−26	−64	11	3.03
20	R Temporal Lobe, Middle Gyrus	21	59	10	−27	3.00
	R Temporal Lobe, Superior Gyrus	38	59	11	−19	2.71
11	L Occipital Lobe, Cuneus	18	−20	−79	17	2.98
12	R Frontal Lobe, Superior Frontal Gyrus	9	6	48	33	2.90

Table 4

Brain areas with significantly ($p < 0.0025$) greater activity during the first (TSB1), second (TSB2), and third (TSB3) applications of either sham or active non-invasive cervical vagal nerve stimulation during trauma as measured with positron emission tomography. Significant clusters are presented by size (number of voxels) and location (Brodmann area, cluster peak Talairach coordinates). Sub-cluster peaks are also identified. ND = no difference.

Voxel Number	Brain Region	Brodmann Area	Talairach			Z Score
			X	Y	Z	
Activation						
TSB2 > TSB1: ND						
TSB3 > TSB2						
11	R Parietal Lobe, Postcentral Gyrus	1	65	−21	38	4.05
12	L Frontal Lobe, Precentral Gyrus	6	−57	6	11	3.86
18	R Putamen		20	4	1	3.63
11	R Temporal Lobe, Superior Gyrus	22	59	4	1	3.25
Deactivation						
TSB2 > TSB1						
28	L Temporal Lobe, Inferior Gyrus	20	−51	−51	−11	3.75
11	L Occipital Lobe, Cuneus	18	0	−85	11	3.31
TSB3 > TSB2						
11	L Occipital Lobe, Precuneus	31	−4	−72	27	3.60
12	R Temporal Lobe, Superior Gyrus	22	53	−48	16	3.52
25	L Temporal Lobe, Middle Gyrus	21	−63	−12	−9	3.47
16	L Occipital Lobe, Precuneus	31	0	−65	20	3.43

Table 5

Brain areas with significantly ($p < 0.0017$) greater activity during the first (TSB1), second (TSB2), and third (TSB3) applications of sham compared to active non-invasive cervical vagal nerve stimulation during trauma scripts as measured with positron emission tomography. Significant clusters are presented by size (number of voxels) and location (Brodmann area, cluster peak Talairach coordinates). Sub-cluster peaks are also identified.

Voxel Number	Brain Region	Brodmann Area	Talairach			Z Score
			X	Y	Z	
TSB1						
21	L Cerebellum		−46	−49	−40	4.37
15	L Cerebellum		−34	−46	−30	4.21
23	L Cerebellum		−26	−36	−17	4.17
23	R Parahippocampal Gyrus		28	−33	−7	3.81
13	L Occipital Lobe, Fusiform Gyrus	37	−36	−41	−8	3.80
58	L Parahippocampal Gyrus		−36	−16	−16	3.77
	L Temporal Lobe, Fusiform Gyrus	20	−44	−19	−23	3.07
	L Parahippocampal Gyrus		−28	−20	−16	3.06
21	R Cerebellum		14	−83	−35	3.76
36	R Temporal Lobe, Inferior Gyrus	20	67	−28	−20	3.58
13	R Limbic Lobe, Uncus	20	34	−9	−30	3.58
24	R Frontal Lobe, Middle Gyrus	10	32	47	−2	3.57
50	R Frontal Lobe, Medial Gyrus	6	12	8	52	3.54
	R Anterior Cingulate	24	4	0	45	3.38
11	R Parietal Lobe, Precuneus	7	8	−35	45	3.42
17	R Cerebellum		20	−40	−22	3.42
32	L Frontal Lobe, Superior Gyrus	10	−20	56	2	3.41
11	R Insula	13	42	−6	5	3.40
13	L Cerebellum		−28	−66	−29	3.27
17	L Frontal Lobe, Rectal Gyrus	11	−6	15	−19	3.23
12	L Frontal Lobe, Inferior Gyrus	46	−44	43	6	3.21
12	L Frontal Lobe, Middle Gyrus	11	−26	36	−12	3.04
TSB2						
41	L Temporal Lobe, Inferior Gyrus	37	−57	−61	−7	5.12

Voxel Number	Brain Region	Brodmann Area	Talairach			Z Score
			X	Y	Z	
11	L Frontal Lobe, Inferior Gyrus	45	−46	22	14	4.40
22	R Cerebellum		26	−50	−24	4.12
23	R Temporal Lobe, Sub-Gyral	21	46	−6	−13	4.06
49	L Limbic Lobe, Anterior Cingulate	24	−10	20	21	3.78
20	R Frontal Lobe, Middle Gyrus	9	28	28	25	3.66
	R Frontal Lobe, Middle Gyrus	9	36	29	30	3.52
17	L Frontal Lobe, Middle Gyrus	8	−26	25	34	3.59
14	R Cerebellum		12	−87	−31	3.58
14	R Temporal Lobe, Medial Gyrus	21	51	−43	0	3.45
TSB3						
17	R Caudate		14	20	9	5.54
118	R Parietal Lobe, Postcentral Gyrus	1	65	−21	38	5.51
	R Parietal Lobe, Inferior Lobule	40	67	−29	33	4.32
	R Parietal Lobe, Inferior Lobule	40	53	−37	45	4.25
18	L Frontal Lobe, Paracentral Lobule	5	−12	−31	48	4.22
47	R Claustrum		26	23	2	4.18
	R Claustrum		30	17	−1	3.90
63	L Frontal Lobe, Middle Gyrus	46	−46	51	8	4.11
	L Frontal Lobe, Inferior Gyrus	46	−48	43	11	3.37
	L Frontal Lobe, Middle Gyrus	10	−38	59	7	3.07
11	R Parietal Lobe, Precuneus	19	8	−80	39	3.77
19	L Claustrum		−34	−9	11	3.72
17	R Parietal Lobe, Superior Lobule	7	34	−68	47	3.64
13	R Temporal Lobe, Fusiform Gyrus	37	51	−45	−13	3.59
12	R Parietal Lobe, Superior Lobule	7	20	−67	52	3.45

Table 6

Brain areas with significantly ($p < 0.0017$) greater deactivations with sham compared to non-invasive cervical vagal nerve stimulation nVNS during the first (TSB1), second (TSB2), and third (TSB3) exposures to personalized trauma as measured with positron emission tomography. Significant clusters are presented by size (number of voxels) and location (Brodmann area, cluster peak Talairach coordinates). Sub-cluster peaks are also identified. ND = no difference.

Voxel Number	Brain Region	Brodmann Area	Talairach			Z Score
			X	Y	Z	
TSB1						
64	R Temporal Lobe, Fusiform Gyrus	37	40	−57	−6	4.66
	R Temporal Lobe, Fusiform Gyrus	37	46	−51	−9	3.12
33	R Parahippocampal Gyrus	30	10	−39	0	4.52
60	R Frontal Lobe, Inferior Gyrus	46	34	17	24	4.44
32	R Parietal Lobe, Postcentral Gyrus	43	63	−11	16	4.27
37	R Limbic Lobe, Posterior Cingulate	30	14	−50	12	4.25
25	L Frontal Lobe, Precentral Gyrus	9	−32	4	35	4.25
25	L Anterior Cingulate	32	−10	32	10	4.14
16	R Posterior Cingulate	30	24	−70	8	3.99
17	R Occipital Lobe, Cuneus	18	12	−71	20	3.75
12	L Frontal Lobe, Inferior Gyrus	45	−53	11	23	3.72
28	L Posterior Cingulate	31	−14	−41	32	3.57
14	R Occipital Lobe, Cuneus	18	16	−84	21	3.56
14	L Temporal Lobe, Middle Gyrus	37	−42	−60	1	3.35
14	R Occipital Lobe, Inferior Gyrus	37	44	−66	−2	3.34
13	R Occipital Lobe, Inferior Gyrus	19	36	−78	−6	3.30
11	R Insula	13	38	−24	20	3.27
TSB2						
43	R Frontal Lobe, Precentral Gyrus	6	50	−2	7	4.58
15	L Parietal Lobe, Precuneus	7	−4	−33	45	4.58
13	R Occipital Lobe, Middle Gyrus	19	32	−90	18	4.55
25	R Insula	13	48	−24	21	4.45
	R Parietal Lobe, Postcentral Gyrus	40	57	−26	23	3.24

Voxel Number	Brain Region	Brodmann Area	Talairach			Z Score
			X	Y	Z	
49	L Frontal Lobe, Middle Gyrus	6	−26	−9	63	4.29
	L Frontal Lobe, Superior Gyrus	6	−18	−6	66	4.00
11	R Insula	13	38	−9	16	4.18
16	L Cerebellum		−32	−45	−16	4.05
14	R Frontal Lobe, Medial Gyrus	10	16	51	6	4.02
14	R Frontal Lobe, Superior Gyrus	6	24	7	58	3.94
13	L Cerebellum		−2	−78	−11	3.91
14	L Frontal Lobe, Superior Gyrus	6	−18	14	56	3.91
14	R Frontal Lobe, Precentral Gyrus	44	63	8	11	3.89
	R Frontal Lobe, Inferior Gyrus	9	67	11	18	3.60
13	L Temporal Lobe, Superior Gyrus	39	−46	−48	11	3.59
11	R Frontal Lobe, Middle Gyrus	9	38	35	35	3.59
14	L Insula	13	−34	6	8	3.56
12	R Thalamus		8	−7	10	3.31
TSB3						
18	L Frontal Lobe, Superior Gyrus	10	−16	51	18	4.57
15	L Frontal Lobe, Middle Gyrus	9	−42	11	35	4.46
18	R Temporal Lobe, Superior Gyrus	38	48	18	−21	4.37
20	R Cerebellum		30	−30	−22	4.34
26	R Frontal Lobe, Medial Gyrus	10	14	45	3	4.21
22	L Occipital Lobe, Precuneus	31	−2	−67	20	3.99
14	R Anterior Cingulate	32	10	35	7	3.76
13	R Frontal Lobe, Inferior Gyrus	47	57	33	−5	3.44
	R Frontal Lobe, Inferior Gyrus	47	61	21	−3	3.18

Table 7

Brain areas with significantly ($p < 0.005$) greater activity during the application of sham non-invasive cervical vagal nerve stimulation (nVNS) and active nVNS during rest as measured with positron emission tomography. Significant clusters are presented by size (number of voxels) and location (Brodmann area, cluster peak Talairach coordinates). Sub-cluster peaks are also identified.

Voxel Number	Brain Region	Brodmann Area	Talairach			Z Score
			X	Y	Z	
Sham > nVNS						
138	L Parietal Lobe, Inferior Lobule	40	−53	−39	27	4.10
	L Insula	13	−44	−41	25	4.08
116	L Parietal Lobe, Precuneus	7	−14	−60	47	4.07
	L Parietal Lobe, Precuneus	7	−8	−72	45	3.47
109	L Temporal Lobe, Middle Gyrus	21	−44	3	−25	3.72
42	R Cerebellum		4	−61	−10	3.67
84	L Frontal Lobe, Medial Gyrus	8	−12	33	35	3.66
	L Frontal Lobe, Medial Gyrus	9	−10	40	32	3.63
68	L Cerebellum		−40	−54	−33	3.58
51	R Frontal Lobe, Medial Gyrus	9	20	44	20	3.49
60	L Frontal Lobe, Middle Gyrus	47	−40	35	−8	3.46
24	L Parietal Lobe, Precuneus	7	−2	−72	34	3.43
16	R Frontal Lobe, Middle Gyrus	46	51	21	22	3.40
23	L Frontal Lobe, Middle Gyrus	11	−22	46	−9	3.39
59	L Cerebellum		−26	−70	−37	3.39
110	L Anterior Cingulate	32	−6	43	5	3.37
	L Frontal Lobe, Medial Gyrus	10	−16	45	5	3.27
	L Anterior Cingulate	32	−16	39	12	2.76
23	R Parietal Lobe, Precuneus	19	30	−80	34	3.35
55	R Frontal Lobe, Medial Gyrus	10	20	51	6	3.27
	R Frontal Lobe, Medial Gyrus	10	12	51	4	2.93
47	L Temporal Lobe, Middle Gyrus	20	−55	−37	−7	3.22
	L Temporal Lobe, Middle Gyrus	20	−50	−34	−10	2.76
15	R Frontal Lobe, Medial Gyrus	10	8	46	−6	3.19

Voxel Number	Brain Region	Brodmann Area	Talairach			Z Score
			X	Y	Z	
26	R Parietal Lobe, Postcentral Gyrus	2	69	−20	26	3.16
11	R Temporal Lobe, Supramarginal Gyrus	40	61	−47	27	3.13
18	L Temporal Lobe, Middle Gyrus	21	−59	−18	−14	3.13
12	R Occipital Lobe, Cuneus	17	16	−87	11	3.08
12	R Anterior Cingulate	32	20	17	36	3.06
35	L Frontal Lobe, Medial Gyrus	10	0	62	0	3.05
	R Frontal Lobe, Superior Gyrus	10	6	60	−6	2.70
47	R Parietal Lobe, Precuneus	7	10	−74	41	3.05
	R Parietal Lobe, Precuneus	7	6	−71	47	2.88
13	R Frontal Lobe, Superior Gyrus	9	8	52	21	3.04
30	R Cerebellum		28	−72	−35	3.03
20	L Insula	13	−40	4	−7	3.01
13	R Cerebellum		16	−58	−39	2.98
12	R Parietal Lobe, Angular Gyrus	39	44	−62	35	2.98
11	L Frontal Lobe, Paracentral Lobule	5	−4	−38	47	2.93
nVNS > Sham						
31	L Occipital Lobe, Inferior Gyrus	17	−14	−92	−6	3.36
63	R Temporal Lobe, Middle Gyrus	37	44	−66	7	3.33
31	L Frontal Lobe, Inferior Gyrus	47	−34	27	−5	3.24
18	R Frontal Lobe, Inferior Gyrus	47	50	42	10	3.17
21	L Temporal Lobe, Middle Gyrus	21	−53	9	−24	2.91